UNIVERSITY OF INDONESIA

BIODISTRIBUTION AND INTERNAL DOSIMETRY OF TECHNETIUM 99M PERTECHNETATE IN THYROID SCINTIGRAPHY: IN VIVO AND PHANTOM STUDY

THESIS

ARRETA REI
0906494990

FACULTY OF MATHEMATICS AND NATURAL SCIENCE
PHYSICS MASTER PROGRAM
MEDICAL PHYSICS AND BIOPHYSICS
JAKARTA
JULY 2011

UNIVERSITY OF INDONESIA

BIODISTRIBUTION AND INTERNAL DOSIMETRY OF TECHNETIUM 99M PERTECHNETATE IN THYROID SCINTIGRAPHY: IN VIVO STUDY AND PHANTOM PRODUCTION

THESIS

Submitted in partial fulfillment of the requirement for the Master of Science degree

ARRETA REI
0906494990

FACULTY OF MATHEMATICS AND NATURAL SCIENCE
PHYSICS MASTER PROGRAM
MEDICAL PHYSICS AND BIOPHYSICS
JAKARTA
JULY 2011

PAGE OF ORIGINALITY STATEMENT

This thesis is my own creation,

and all of citations and references have been stated

by me correctly.

Name	: Arreta Rei
Student Number (NPM)	: 0906494990
Signature	:
Date	: 14 July 2011

PAGE OF ENDORSEMENT

This thesis was submitted by :
Name : Arreta Rei
Student Number (NPM) : 0906494990
Study Program : Physics
Major : Medical Physics
Title : Biodistribution and Internal Dosimetry of Technetium 99m Pertechnetate in Thyroid Scintigraphy: In Vivo and Phantom Study

Has been examined by examiner board and accepted as the fulfillment of the requirement for the Master of Science degree in Master Program of Physics, Major of Medical Physics and Biophysics, Faculty of Mathematics and Natural Sciences.

EXAMINER BOARD

Supervisor :Prof. DR. Djarwani S. Soejoko (....)

Examiner I : DR. Musaddiq Musbach (....)

Examiner II : DR. Seruni U. Freisleben (....)

Examiner III : Prof. Kwan Hong Ng, PhD. (....)

Passing examination at : Jakarta
Date : 14 July 2011

PREFACE

Praise to Allah Almighty for the guidance, blessing, inspiration, and ease, so that this thesis could be done. Many support and help were received by me during this hard work. Therefore I would like to extend gratitude to:

- Prof. DR. Djarwani S. Soejoko as my supervisor for her time and widely knowledge. I learn very much from her, and it was really an honor to have her as my supervisor.
- DR. rer. nat. Musaddiq Musbach, DR. Seruni Udyaningsih Freisleben, and Prof. Kwan Hong Ng, PhD. for being my examiners and giving me precious advices for this thesis revision.
- Lectures and administration staffs of Physics Department, University of Indonesia.
- Pertamina Center Hospital, especially Nuclear Medicine Installation doctors and staffs, Dr. Chafied Varuna, Sp.KN as the head, Dr. Fadhil Nazir, Sp.KN for many advices, Mr. Tetra, Mr. Erwin Firmansyah, Mr. Duta Kamesworo, and each of you that I couldn't mention one by one. Thanks for your help and assistance.
- My beloved mother Natasha Erwinn and my beloved sister Marsha Ceniza for encouraging and giving me big attention during finishing this thesis.
- My seniors, but also my colleagues, Kristina Tri Wigati, M.Si, Dwi Seno, M.Si, and Supriyanto, M.Si. Big thanks for attention and be understanding of a situation while I am doing this thesis.
- My friends in Medical Physics Master Program 2009, especially for Rini Suryanti for this very nice struggle. Surely we can pass through all of these moments.
- Hardiani Rahmania, S.Farm for giving me wonderful life of each days.
- My juniors in college, Lukmanda Evan Lubis, Melati Azizka, Yakub A. Bayhaqi, Purwinda Herin M., ADZEM circle's, and Fenny Febrianita for helping me and bringing the colorful days to me.

- Each of you that involved during my study and thesis work, although I could not mention each.

May Allah bless all of you. I hope this thesis could be worthwhile for nuclear medicine development and observation. I realized that this thesis is not perfect, therefore constructive advices are needed for this improvement. Thank you very much.

Author

2011

PAGE OF THESIS PUBLICATION AGREEMENT FOR ACADEMIC UTILITY

As the academics member of University of Indonesia, I, The undersigned below

Name	: Arreta Rei
Student Number (NPM)	: 0906494990
Degree Program	: S2 (Master)
Departement	: Physics
Faculty	: Mathematics and Natural Sciences
Kind of Creation	: Thesis

for knowledge development, I agree to grant to University of Indonesia ***Non-exclusive Royalty Free Right***of my scientific creation with title : Biodistribution and Internal Dosimetry of Technetium 99m Pertechnetate in Thyroid Scintigraphy: In Vivo and Phantom Study

So that, University of Indonesia have the right to preserve, to media convert, to manage in database, and to publish my thesis as long as put my name as the author/creator and the copyright owner.

This statement was made by me correctly.

Made at: Depok

Date: 14 July 2011

Stated by

(Arreta Rei)

ABSTRAK

Nama : Arreta Rei
Program Studi : Fisika
Kekhususan : Fisika Medis
Judul Tesis : Bioditribusi dan Dosimetri Internal Technetium 99m Pertechnetate dalam Skintigrafi Tiroid: Studi In Vivo dan Fantom

Telah dilakukan penelitian uji biodistribusi dan dosimetri Tc-99m perteknetat dalam tubuh yang bertujuan untuk mengetahui alir Tc-99m dalam metabolisme dan prediksi dosis internal dan eksternal yang diterima pasien skintigrafi kelenjar tiroid. Penelitian dilakukan dengan melakukan pemindaian berulang dengan pencitraan planar AP dan PA pada lapangan leher, toraks abdomen, dan pelvis dalam suatu interval waktu hingga 90 menit setelah penyuntikan terhadap pasien skintigrafi kelenjar tiroid. Biodistribusi Tc-99m perteknetat menunjukan persentase yang tinggi pada jantung, liver, dan ginjal pada rentang 0-10 menit pertama, sedangkan pada rentang waktu 30 – 40 menit dan 60 -70 menit persentase tertinggi terjadi pada lambung.Penghitungan dosis internal menunjukkan 7.4 x 10^{-1} mGy/mCi pada kandung kemih, 3.38x 10^{-2} mGy/mCi pada tiroid, 9.15 x 10^{-2} mGy/mCi pada lambung, 3.33 x 10^{-2} mGy/mCi pada ginjal, 3.10 x 10^{-2} mGy/mCi pada jantung, and 1.5 x 10^{-2} mGy/mCi pada hati. Untuk pengukuran dosis eksternal (Surface Dose) dengan menggunakan TLD, diperoleh laju dosis setiap menitnya untuk tiroid, lambung, dan kandung kemih berturut-turut: 3.33 x 10^{-3} mGy/mCi menit, 3.54 x 10^{-3} mGy/mCi menit, dan 3.32 x 10^{-3} mGy/mCi menit. Desain fantom dinamik tiroid berdasarkan pada metabolisme Tc-99m perteknetat dalam tiroid pasien sehat, memberikan hasil yang baik dalam menunjukan pengukuran konstanta laju eliminasi dan dosis internal.

Kata kunci : Tc-99m perteknetat, skintigrafi, biodistribusi
xiii + 74 halaman ; 29 Gambar; 10 Tabel; 10 Lampiran
Daftar Acuan : 28 (1987-2010)

ABSTRACT

Name : Arreta Rei
Study Program : Physics
Major : Medical Physics
Title : Biodistribution and Internal Dosimetry of Technetium 99m Pertechnetate in Thyroid Scintigraphy: In Vivo and Phantom Study

The study of biodistribution and dosimetry testing for Tc-99m pertechenetate has been done to asses its flow in metabolism and predict internal and external patients dose. Thyroid scintigraph patients were periodically scanned with AP and PA planar imaging on neck, thorax abdomen, and pelvic field for several interval times up to 90 minutes after Tc-99m pertechnetate injected. Biodistribution shows the highest activity percentage in the heart, liver, and kidney at period 0 – 10 minutes, whereas in the stomach at period 30 – 40 minutes and 60 – 70 minutes. Internal dose calculation shows 7.4 x 10^{-1} mGy/mCi for bladder, 3.38x 10^{-2} mGy/mCi for thyroid, 9.15 x 10^{-2} mGy/mCi for stomach, 3.33 x 10^{-2} mGy/mCi for kidney, 3.10 x 10^{-2} mGy/mCi for heart, and 1.5 x 10^{-2} mGy/mCi for liver. External dose with TLD measurement obtained dose rate per minute for thyroid, gastric, and baldder respectively are3.33 x 10^{-3} mGy/mCi min, 3.54 x 10^{-3} mGy/mCi min, and 3.32 x 10^{-3} mGy/mCi min. Dynamic thyroid phantom designing based on health patient thyroid metabolism of Tc-99m pertechnetate gave good results in performing elimination rate constant and internal dose measurement.

Keyword : Tc-99m pertechnetate, scintigraph, biodistribution
xiii + 74 pages: 29 Figures; 10 Tables; 10 Appendices
References : 28 (1987-2010)

CONTENTS

LIST OF FIGURES

LIST OF TABLES

LIST OF APPENDIX

CHAPTER 1
INTRODUCTION

1.1 Background

Thyroid scintigraphy with Iodine 131 was left in clinical practice in early 1990. Just for some cases, I-131 was used for diagnostic. This modality has been subtituted by using radiophamaceutical Tc-99m pertechnetate labeled with MIBI (methoxy-isobutil-isonitrile) (Kresnik, Gallowitsch, Mikosch, Gomez, & Lind, 1997; Saber, Wagih, Sedik, & Fawzy, 2001). Fast scan of thyroid uptake could be done by using Tc-99m MIBI, even early image scanning perfomed better result than late image (Yokoyama N., et. al., 1986). Therefore, it is more effective than I-131 that needs 24 hours to do scanning after injection (Saber, Wagih, Sedik, & Fawzy, 2001).

Nowadays, there are many clinical practices using Tc-99m pertechnetate non label. Physicians accept these image results to diagnose for several thyroid abnormalities. The retention time of Tc-99m pertechnetate is shorter than Tc-99m MIBI because there is no organ binding tendencion. Other advantage of this use is the low cost because it does not require the labeling kit. Quantitive data for this use is required to perform the radiopharmaceutical flow in human body and the dose received by several organs.

Different from radiology and radiotherapy, nuclear medicine have radiation retention time. Even though after the clinical examination, the patients still containt radioisotope material that irradiate for several times, not only in the target organ but also other organs. Internal and external dose measurements were performed in this study. Internal dose measurement was subjected to predict absorb dose received by organs. In some cases, thyroid scintigraphy is the frequently examination to monitor the treatment result. So that, it was needed to calculate the internal dose. External dose measurement related with radiation protection for public that is contributed from patient of this modality.

Internal dose measurement and image optimization testing in nuclear medicine needs human metabolism because it depends on uptake and elimination flow of the radiopharmaceutical. Therefore, patients must be involved in every kind of investigation. The measurement method is not comfortable for the patients because it has to do scanning repeatedly, so takes longer time than the clinical procedure that need for the examination. Even in using MIRDOSE 3.1 software to calculate internal dose, it also requires residence time from patient measurement (Stabin M. G., 1996). A dynamic phantom which represents an organ flow of Tc-99m pertechnetate in human metabolism is needed to be a solution of this problem. Thyroid dynamic phantom was made in this study. In future, this phantom could be used for other study of image optimization and also for education practice in nuclear medicine.

1.2 Objectives

Several aims of this study, as follows

1. To obtain the informations of Tc-99m pertechnetate biodistribution flow.
2. To quantify internal dose of several organs of thyroid scintigraphy examination.
3. To assess external dose of several organs of thyroid scintigraphy examination.
4. To make a Dynamic Thyroid Phantom and verify it.

1.3 Hypothesis

This study is based on several initial hypotheses, as follow:

1. Effective half life of Tc-99m pertechnetate in thyroid between 0.86 – 3.76 hours (ICRP, 1987).
2. The highest dose was received by stomach, and followed by thyroid, bladder, then other organs (AAPM, 1992).
3. Effective dose equivalent of total body from this examination for each patient was less than 1 mSv (Harding, 2001; UNSCEAR, 2008).

1.4 Problem Limitation

This study was limited in Tc-99m pertechnetate used for thyroid scintigraphy modality in point of view biodistribution and dosimetry, without consideration of its drugs binding and chemical structure. The dynamic phantom was made just to simulate Tc-99m pertechnetate elimination flow in normal thyroid.

CHAPTER 2
THEORY

2.1 Biodistribution

The determination of radiation dose from radionuclides within the body and the calculation of amounts that may be safely inhaled or ingested depend on knowledge of the fate of these radionuclides within the body. Specifically, it needs to know the pathways, the rates at which they travel along these pathways, and the rates at which they are eliminated from the body (Cember, 1994). Therefore, biodistribution is very important in internal dosimetry study. By knowing the kineticks of metabolism of a radionuclide, that is, the relationship among exposure, intake, uptake, deposition, and excretion of a radionuclide, the radiation dose from given exposure can be calculated (Cember, 1994).

Although radiopharmaceuticals have the specific organ receptor in human body, it also would be uptaked by other organs which are not the examination target. It may be happened because of the drug binding between the radiopharmaceutical with any organ compounds. Radiopharmaceutical elimination in the body described by an exponential decay process that containts physical half life and biological half life, the analogous term of both is effective half life ($T_{e1/2}$). Effective half life is defined as time required for one –half of a given quantity of a radionuclide to be cleared from the body or from a specified organ of the body via physiological and biokinetic process (Raabe, 1994).

To simulate organ in absorbtion and elimination process, it was common to use compartment model. Compartment is organ or system organ with the same of blood track and drug affinity (Shargel & Yu, 2005). The basic was one compartment model as follows

$$A_t = A_0 e^{-kt} \qquad (2\text{-}1)$$

Where A_t is activity (curie) at t (hour); A_0 is activity at t = 0; and k is elimination rate.

The value of k (/hour) and $T_{1/2}$ (hour) could be calculated with this equation (Shargel & Yu, 2005)

$$k = \frac{\ln(C_{t,1}) - \ln(C_{t,2})}{t_2 - t_1} = \frac{\ln(A_{t,1}) - \ln(A_{t,2})}{t_2 - t_1} \qquad (2.2)$$

$$T_{1/2} = \frac{\ln 2}{k} \qquad (2\text{-}3)$$

where C is concentration, since this equation was used to calculate the elimination rate, the quantity could be change as long as it represents the same function.

2.2 Internal Radiation Dosimetry

Internal radiation dosimetry is the scientific methodology used to measure, calculate, estimate, assay, predict, and otherwise quantify the radiative energy absorbed by the ionization and excitation of atoms in human tissue as a result of the emission of energetic radiation by internally deposited radionuclides (Raabe, 1994). Internal radiation quantification could not be measured, but calculated (Chiesa, 2010). The radiation doses received by tissues of the body must be computed in assessments of the potential health detriment associated with exposures to ionizing radiations (Eckerman K. F., 1994).

Dosimetry studies are subjected to determine the fundamental relationships between energy deposition in biological tissues and resulting endpoints (radiation-induced damaged, or biochemical changes) (Fisher, 1994). The mean absorbed dose expressed in rads to a target organ r_k from a radionuclide distributed uniformly in a source organ r_h has been formulated by the MIRD Committee (Snyder, Ford, Warner, & Watson, 1975) as

$$\overline{D}_{(rk \leftarrow rh)} = \frac{\tilde{A}_h}{m_k} \sum \Delta_i \phi_{(rk \leftarrow rh)}$$

$$S_{(rk \leftarrow rh)} = \frac{\sum \Delta_i \phi_{(rk \leftarrow rh)}}{m_k}$$

$$\overline{D}_{(rk \leftarrow rh)} = \tilde{A}_h S_{(rk \leftarrow rh)} \qquad (2\text{-}4)$$

where $\tilde{A}_h$ (µCi hr) is the cumulated activity in source organ r_h, m_k (gm) is the mass of target organ r_k, Δi (gm rad/µCi h) is the equilibrium dose constant for particles of a particular type and energy, here indicated by i, and $\phi_{(rk \leftarrow rh)}$ represents the absorbed fraction of energy for target organ r_k for particles i emitted in source organ r_h. The cumulative activity was calculated by integrate the cumulated source activity in organ at the period as follows

$$\tilde{A}_h = \int_{t_1}^{t_2} A_h(t)dt \qquad (2\text{-}5)$$

The activity of organ was obtained by using the mean geometric (MG) equation and involve the conversion factor of count rate to activity (Chiesa, 2010) as follows

$$MG = \sqrt{C_A \times C_P} \qquad (2\text{-}6)$$

$$A = \sqrt{I_A . I_P} . e^{\mu d} . \frac{1}{C} = \sqrt{(I_A \times CF_A).(I_p \times CF_P)} \qquad (2\text{-}7)$$

where C_A and I_A refer to the count value from the image of the anterior position, whereas C_P and I_P are the posterior.

The effective dose equivalent H_E was developed in radiation protection to provide a single dosimetric quantity related to risk of stochastic effects regardless of the distribution of dose among the organs of the body (AAPM, 1992). Because of in radiation particles that involved in nuclear medicine diagnostic have radiation weighting factor (w_R) is 1 (Trueblood, 1991), it commons to neglect the H_T calculation, then directly to H_E calculation. The EDE value was calculated by using this equation (Kereiakes, Williams, Cristy, & Eckerman, 1992)

$$H_E = \sum w_T H_T \qquad (2\text{-}8)$$

Where w_T is tissue weighting factor that performed in ICRP 53 (ICRP, 1987).

2.3 Technetium 99m

Radioactivity is the spontaneous disintegration of the nucleus of the radioactive atom (Lange, 1988). The most common use of Tc-99m is in nuclear medicine, primarily in diagnostic imaging procedures (Barrall, 1992). Production of Tc-99m is based upon the decay of Mo-99 to Tc-99m. As the Mo-99 decays, 89% of the transormations results in production of Tc-99m which is then available for use (Williams, 1992).

The half life of Tc-99m is 6.007 hours. It should be noted that a small quantity of the long lived Tc-99 will be present wherever Tc-99m decays (Barrall, 1992). The decay scheme is shown in Figure 2.1

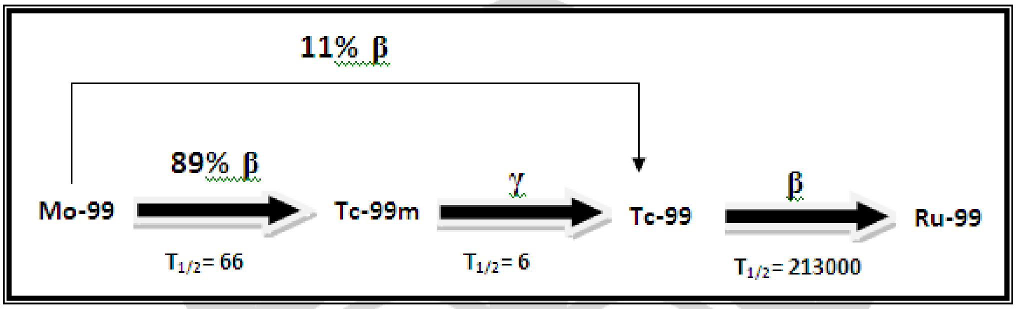

Figure 2.1 Decay scheme for Mo-99 – Tc-99m

Tc-99 is a direct product of the decay of Mo-99 in 12.4% of the Mo-99 decays. Tc-99 also results from most decays of Tc-99m, meanwhile Tc-99m decays to Ru-99 in 0.000098% of its decays. The remainders of the decays of Tc-99m are to Tc-99, which is also radioactive (Barrall, 1992). Mo-99 generator is shown in Figure 2.2.

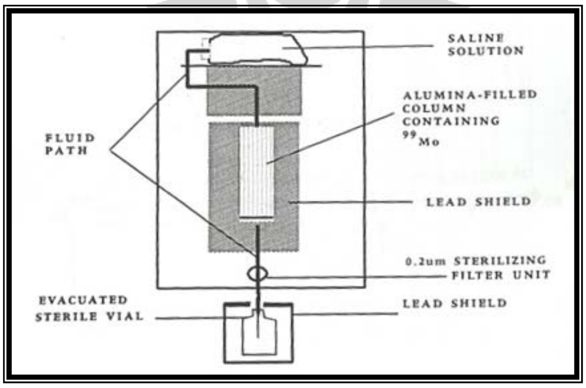

Figure 2.2 Generator model of Mo-99 – Tc-99m (Williams, 1992)

The eluted pertechnetate from a generator may be used directly as a radiopharmaceutical in patients as prescribed by the nuclear medicine physician.

Package inserts from generator indicate that the pertechnetate may be used for imaging the brain, thyroid, salivary glands, blood pool, bladder, the vasolacrimal drainage system, and localizing the placenta. The pertechnetate impurities concentrated primarily in the Gastro-Intestine (GI) tract, the salivary gland, and the thyroid gland, so that these organs will appear on the resulting nuclear medicine images (Williams, 1992).

2.4. Gamma Camera

The gamma camera (also named Anger camera) is the instrument for imaging both static and dynamic radionuclides distribution in vivo (Muehllehner, 1988; Simsons, 1992). Gamma camera diagram adapted from the 1958 publication by Anger is shown in Figure 2.3.

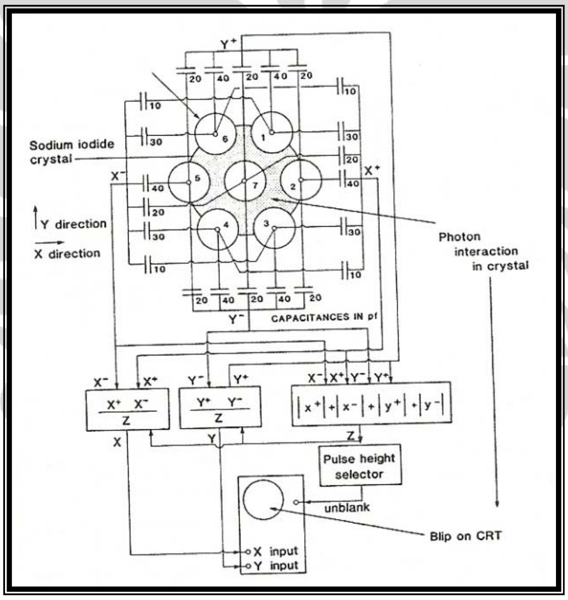

Figure 2.3 First gamma camera model (Simsons, 1992)

The gamma camera has 3 basic components: the scintillation crystal that converts the energy of gamma photon into visible light, the photomultiplier tube (PMT) that converts the light into electronic pulse, and the processing unit that amplifies the pulse, by means of pulse height analysis, select it for recording or rejects it (Oppenheim & Beck, 1988).

The instrument uses the large diameter (25 – 40 cm) sodium iodide crystal optically coupled to an array of PMTs to localize gamma ray interactions in two dimensions. The crystal is thin (6-10 mm) to minimize resolution degradation from multiple scattering interactions within the crystal. The output of each PM tube is weighted by a fixed capacitor or resistor according to its position in array (Simsons, 1992).

A high energy photon entering the scintillation crystal may pass through it without interacting or may interact with and transfer energy to one of the electrons within the crystal, either by a photoelectric or by a Compton interaction (Oppenheim & Beck, 1988). Figure 2.4 shows this incident.

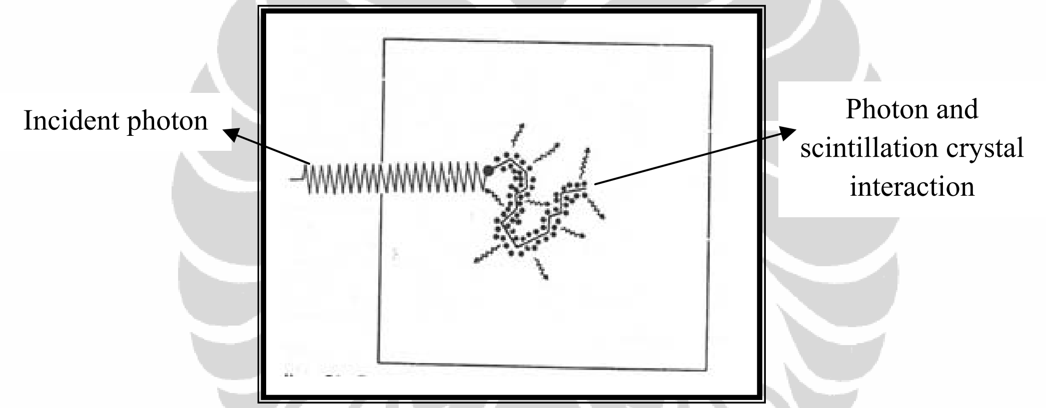

Figure 2.4 Interaction between photon and scintillation detector (Oppenheim & Beck, 1988)

Because of the sensitivity of the PMTs to magnetic fields, metal is used to shield individual tube. The entire detector assembly is heavily shielded with lead to virtually eliminate the interaction of radiation from extraneous sources with NaI(Tl) crystral (Graham, 1991). The position of individual events is determinded by feeding tresholded signals from each PMT into the position logic circuit (Kulberg, van Dijk, & Muehllehner, 1972). These signals are then divided by the Z signal to remove the dependence of image size on photon energy. Simultaneous with position encoding, the signals from all of the PMTs are summed without thresholding to determine photon energy (Z pulse) (Graham, 1991).

2.5 Thyroid Scintigraphy

The thyroid gland is located on the front and sides of the trachea just below the larynx. Its two lobes are connected by a middle piece called the isthmus. This gland produces thyroxine (T4), triiodothyronine (T3), and calsitonine. Overall, thyroid involves in regulation of energy production and protein synthesis, which contribute to grow of the body and to normal body functioning throughout life (Scanlon, V. C. & Sanders, T., 2007).

Scintigraphic imaging plays an important role in determining function of thyroid nodules, detecting occult thyroid lesions, localizing ectopic thyroid tissue, and evaluating metastases from papillary-follicular thyroid carcinoma (Sarkar, S. D., 1988).

Current clinically use of Tc-99m pertechnetate takes advantage of its biological properties and biokinetics which resemble somewhat those of iodide. It is concentrated by the thyroid gland, the gastric mucosa, and the salivary glands. These characteristic made Tc-99m pertechnetate suitable for imaging the thyroid and salivary glands, and to assess existence of gastric mucosa.Thyroid imaging with Tc-99m pertechnetate is used mainly for detection of various conditions that displace the normal thyroid cells and result in areas of absent radionuclide uptake. The initial concentration of Tc-99m pertechnetate in thyroid provides significant flux of gamma emissions for imaging. Since Tc-99m pertechnetate is not incorporated into the hormone it can not be used to measure the degree of thyroid function (Ulloa, 1992). Some thyroid scintigraphy images with Tc-99m pertechnetate administered are shown in Figure 2.5.

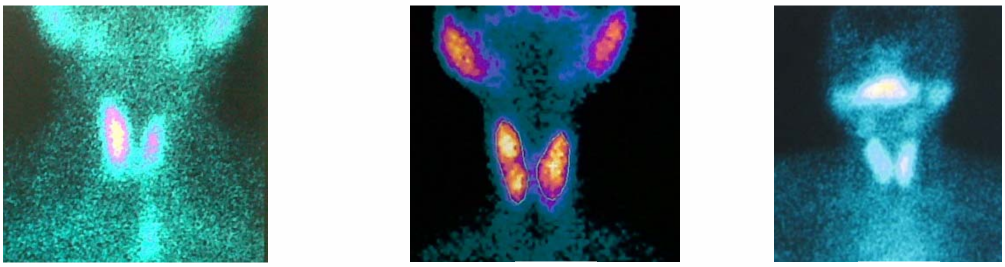

(a) (b) (c)

Figure 2.5 Thyroid scintigraphy images. a. Normal thyroid. b. Hyperthyroid. c. Cold nodule at right thyroid

CHAPTER 3
MATERIALS DAN METHOD

3.1 Flow Chart

This research methodology was divided into four steps, i.e. calibration, biodistribution study, phantom fabrication, and dosimetry study. The flow chart is shown in Figure 3.1.

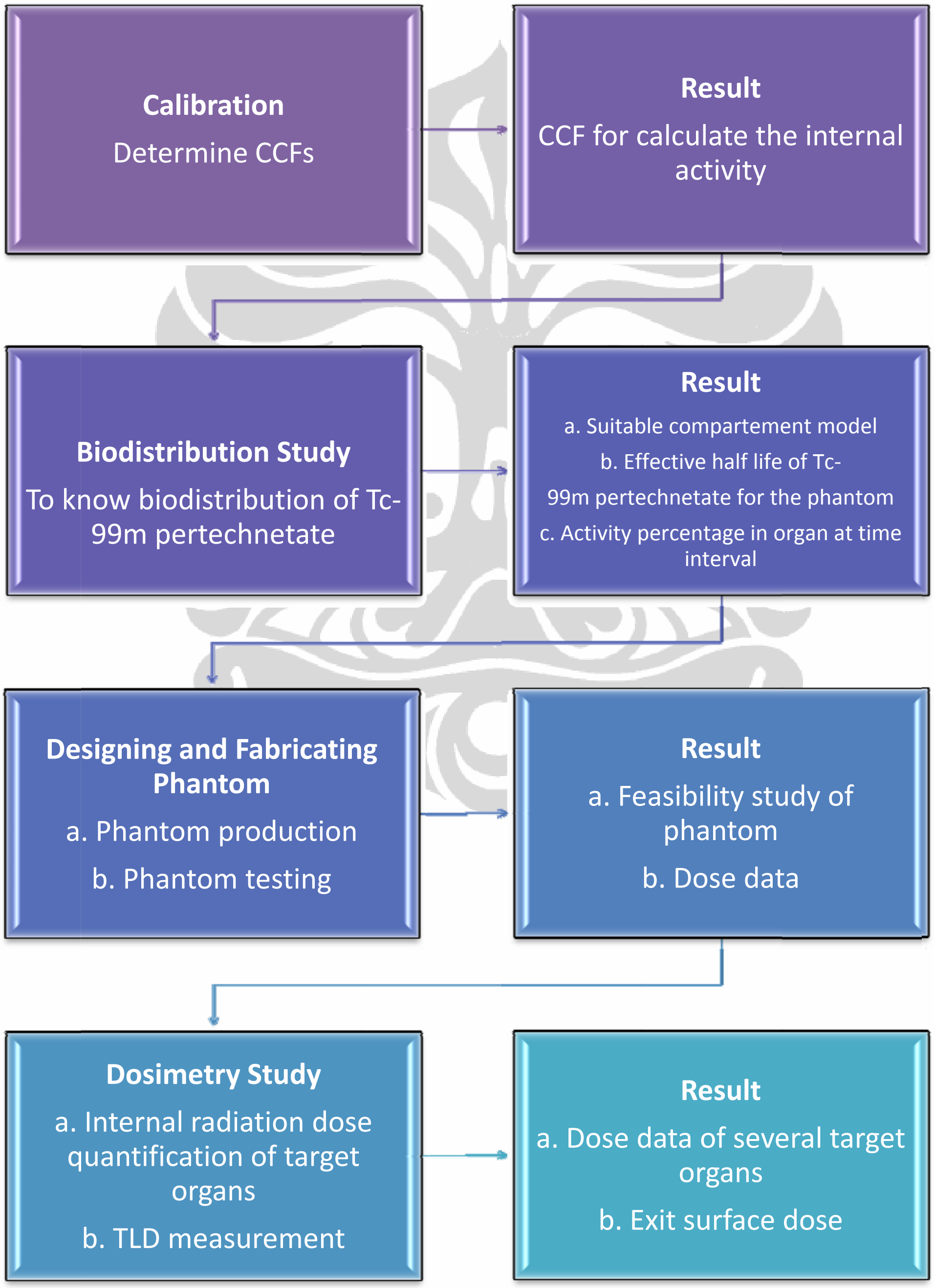

Figure3.1 Research methodology flow chart

3.2 Materials

This study was done at Nuclear Medicine Installation, Pertamina Center Hospital (RSPP), Jakarta, using SPECT unit SKYLight ADAC, Philips, shown in Figure 3.2.

Figure 3.2 Photograph of SPECT unit SKYLight ADAC, Philips

This whole study was conducted by using Low Energy General Purpose (LEGP) collimator for scanning. Measurement of radiopharmaceutical activity was done by using dose calibrator Capintec type CRC-15R, with image processing Pegasys Blade from ADAC. Special 10 cc syringe used for patients and calibration mesurement during this study.

CCFs (mCi/cps) were obtained by measurement using Capintec neck phantom (Figure 3.3) for Thyroid gland and acrylic (methyl methacrylate) blocks for other organs. A ruler was used to measure the thickness of the acrylic, the distance between detector and scanned object, also for other needs.

Figure 3.3 Photograph of Capintec neck phantom

To simulate thyroid gland uptake and elimination, special phantom was made in house with dimension 10 cm x 15 cm x 12 cm (Appendix I), where inside this block there are two cylinders as thyroid gland model. Total volume of cylinders is 13.4 mL (Yokoyama & et., 1986). This phantom is equipped with inlet and outlet ducts that have two faucets to control water debit for being suitable to human elimination phase in metabolism. This phantom is named Dynamic thyroid phantom. The design and photograph of the phantom are showed in Figure 3.4.

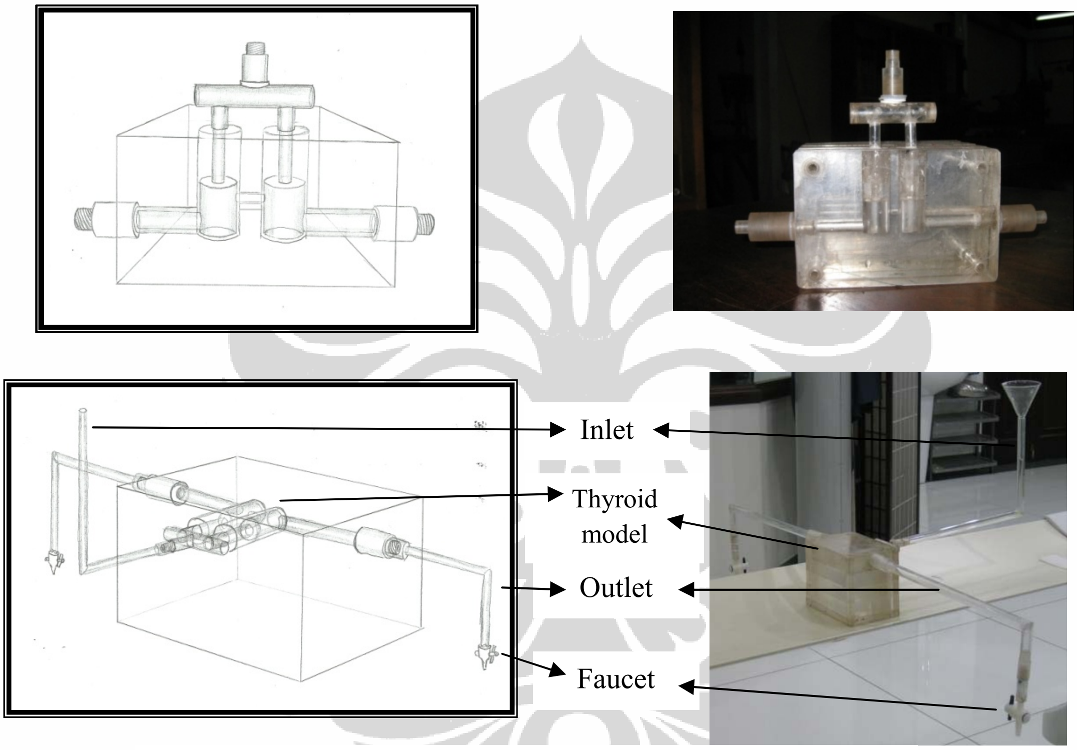

Figure 3.4 Dynamic thyroid phantom and the design

External dose or surface dose was measured with Thermoluminisence Dosimeters (TLDs), Harshaw TLD 100, with each dimension is 3.175 mm x 3.175 mm x 0.9 mm. These TLDs have been calibrated to Tc-99m energy. Reading process was done in Medical Physics Laboratory, Department of Physics, Faculty of Mathematics and Natural Sciences, University of Indonesia.

In this study 21 patients (14 female and 7 male, 18 – 57 years old) were involved, all sample patients were adult either male or female, and subjected to thyroid scintigraphy examination using Tc-99m pertechnetate non labeled. Hyperthyroid and post thyroidectomy patients were not selected.

3.3 Methods

3.3.1 Organ Conversion Factor

For obtaining organ CCFs, information about the organs depth from Anterior-Posterior (AP) and Posterior-Anterior (PA) was required. For this purpose, CT images from 20 patients were observed. All CT images were taken from Treatment Planning System (TPS) data Radiotherapy Installation, Pertamina Center Hospital, Jakarta. The depth measurements were performed by using computer workstation. The result was used to determine the shape and dimension of the CF calibration phantom. This phantom was made suitable to organ position in the human body from anterior and posterior. This is important for the requirement of planar imaging modality that was used in this study. Organ data contain thyroid, heart, liver, kidney, bladder, and stomach can be seen at Appendix A.

Phantom in stack of acrylic layers was used for measurement to obtain organ conversion factors. Syringe filled with Tc-99m pertechnetate was located at the depth which is matchedwith the position of interest organs. Count rate at the surface phantom was collected using SPECT unit with planar modality. The result was displayed on the monitor. The source activities were varied from 1 to 5 mCi with 1 mCi intervals. The interest organs were thyroid, heart, liver, stomach, kidney, and bladder. In case of thyroid, measurements were performed using Capintec neck phantom. Each measurement was repeated up to 3 times. Scheme of this measurement was performed by Figure 3.5.

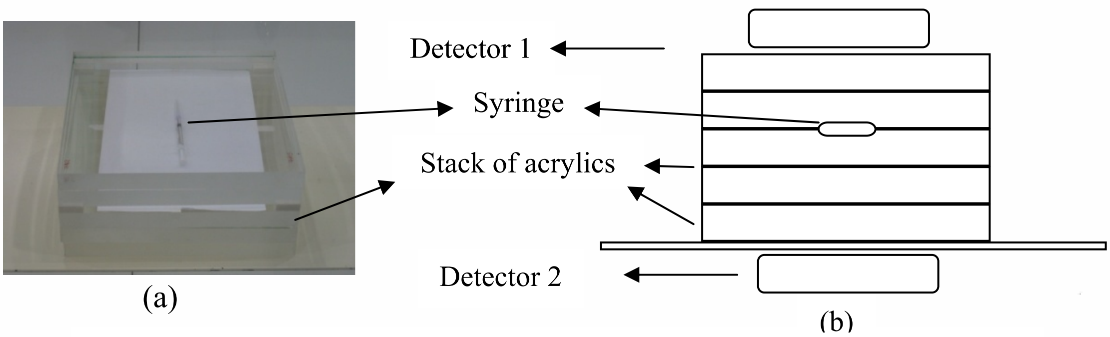

Figure 3.5 Scanning process of calibration. (a) Photograph from above. (b) Phantom cross section

3.3.2 Biodistribution Study

This study was initiated by measuring thyroid gland uptake and elimination of Tc-99m pertechnetate by thyroid gland. Three patients were selected and given about 2-3 mCi Tc-99m pertechnetate. For thyroid gland uptake measurement, image was taken every 2 minutes interval within 20 minutes with dynamic scanning. After this process, image was obtained at longer interval at 30, 60, 90, and 120 minutes after injection by static scanning. It was taken 3 minutes scanning for each time. The curve that was obtained from those scanning could be used to determine the compartement model of Tc-99m pertechnetate elimination in human body. A curve that was obtained from the thyroid scanning give value of Tc-99m pertechnetenat effective half life in human body that obtained from calculating with equation (2-1) and (2-2). This data would be used in dynamic thyroid phantom designing and fabricating. Scanning illustration is showed in Figure 3.6.

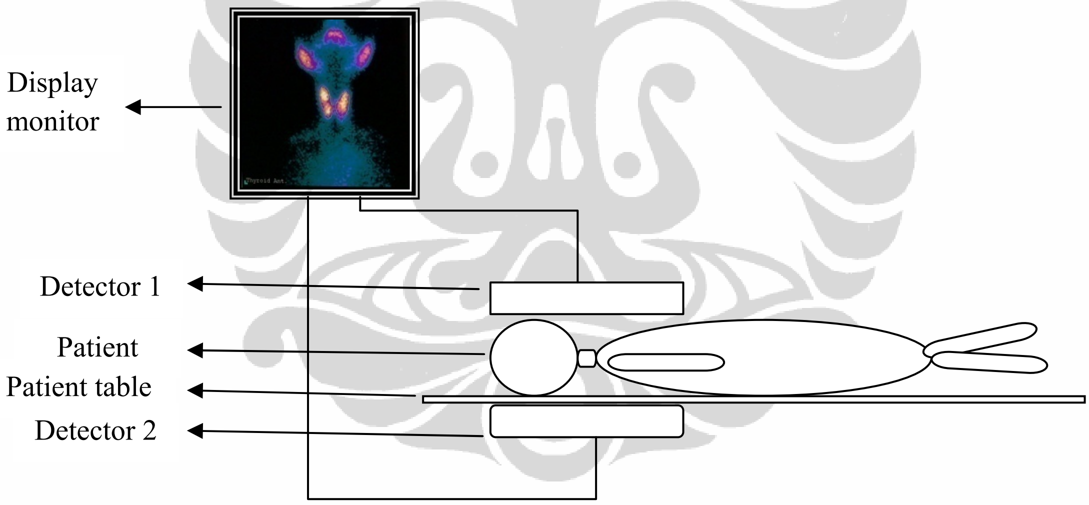

Figure 3.6 Scheme of patient scanning

Biodistribution of Tc-99m pertechnetate in various organs were studied by scanning patients at period 0-10 minutes, 30-40 minutes, 60-70 minutes, and 90-100 minutes after injection. Dynamic scanning was done for thorax abdomen field (heart, liver, stomach, and kidney) every 36 minutes within first 3 minutes, followed by static scanning for neck (thyroid gland, parotic gland, and nasal) and pelvic field (bladder) at mentioned time. Each scanning was done for 3 minutes counting. Planar imaging for AP and PA was used, and energy window was set

20% for 140,5 keV. Count rate at various organ were displayed automatically when Region of Interest (ROI) was determined. Figure 3.7 was showed planar image of several organs with ROI.

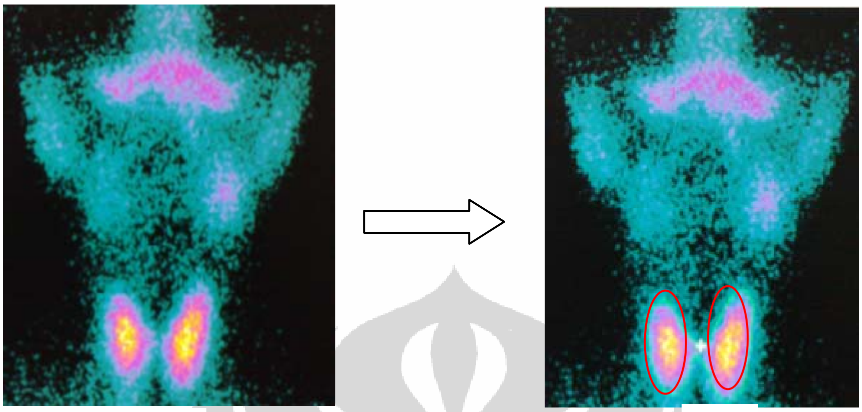

(a) (b)

Figure 3.7 Illustration of ROI determination of thyroid to obtain count rate value. a. Before ROI drawing. b. After ROI drawing

Value of counts in ROI could be obtained from the image processing. Mean geometric from the counts could be calculated by equation (2-6). And finally, activity of the organ was calculated with equation (2-7). Tc-99m pertechnetate biodistribution was expressed in activity percentage with heart as the refrence organ, because as the primary circulatory organ, it accepts the biggest amount of Tc-99m pertechnetate at a few minutes from injection.

3.3.3 Dosimetry Study

MIRD method was used to calculate the internal dose, using the formula which containts S "Snyder" value (Snyder, Ford, Warner, & Watson, 1975) and equation (2-4).

External dose measurement was done by putting TLDs on patient skin, at the region of thyroid gland, stomach, and bladder. Surface dose was calculated from TLDs reading results with this equation

$$D = M \times (TLD)CF \qquad (3\text{-}1)$$

where M is the quantity from TLD reading (nC), and (TLD)CF is TLD conversion factor (mGy/nC).

3.3.4. Phantom Testing

Finally, this study was to test Dynamic Thyroid Phantom. The data collection was performed with the same methods as patient observation. Since this phantom simulates human thyroid gland, therefore, elimination rate constant calculation is the same as those carried out in patients. Then, calculating of the dose also was done with the same methods as the patient. Phantom testing is shown in Figure 3.8.

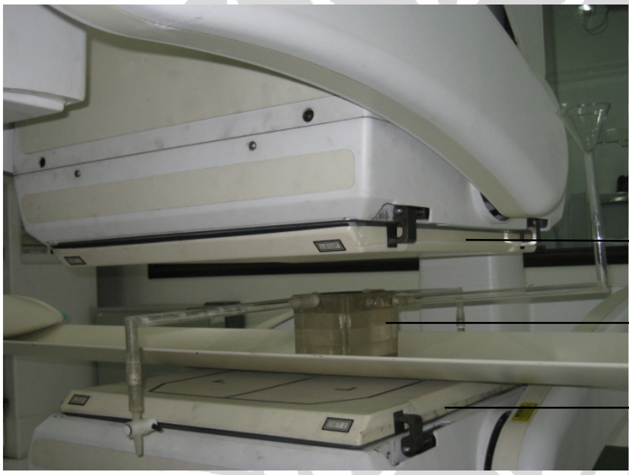

Figure 3.8 Dynamic thyroid phantom testing with SPECT unit

CHAPTER 4
RESULTS AND DISCUSSION

4.1 Result

4.1.1 Calibration

All results of measurement with phantom in various simulated organs are shown at appendix B. From these data, the conversion factors of several organs were obtained and indicated in Table 4.1.

Table 4.1 Count rate conversion factor for each organ and position

Organ	**Count rate CF (mCi/cps)**	
	AP	PA
Heart	3.72E-04	8.61E-04
Liver	2.66E-04	4.02E-04
Kidney	7.02E-04	4.17E-04
Bladder	3.55E-04	8.63E-04
Stomach	5.69E-04	4.41E-04
Thyroid	2.36E-04	9.56E-04

The differences of AP and PA CCFs were due to position of the organs, depend on the depth from the skin surface. AP depth of heart, liver, bladder, and thyroid gland is lower than its PA depth, therefore the CCF will be smaller. The contradictive condition was happened for kidney and stomach.

4.1.2 Biodistribution Study

For biodistribution study, scanning time was determined at 3 periods: 0-10 minutes, 30-40 minutes, and 60-70 minutes after injection. The measurement results can be seen at Appendix D. Mean percentage of T-99m pertechnetate activity in several organs from 21 patients was illustrated in Table 4.2. Percentage values that are normalized respect for activity percentage in heart at period 0-10 minutes (33.33%), named biodistribution percentage; whereas ratio percentage of organ uptake and administered activity was named activity percentage.

Table 4.2 Biodistribution percentage of Tc-99m pertechnetate

Organ	%Biodistribution in time interval		
	0-10 min	30-40 min	60-70 min
Thyroid	3.46	3.89	3.72
Parotic	4.46	2.90	2.51
Nasal	0.95	1.74	2.39
Heart	100.00	34.88	26.46
Liver	53.57	25.12	-
Stomach	8.65	34.43	36.21
Kidney	23.23	2.71	-
Bladder	1.08	8.28	5.42

At the period 0-10 minutes after injection, the flow of Tc-99m pertechnetate is starting from heart (100%) to liver (53.57%) and to kidney (23.23%), while in the other organs mostly unless than 50%. This result supported thatthe biodistribution flow of a substance in metabolism, through the heart, liver, and then flow to other organs which are receptors (Shergel, 2005). After distribution, that substance would be metabolized in kidney to be excreted as urine.

Elimination occurred at period 30-40 minutes, it is indicated the fastest elimination at heart (100% - 34.88%), followed by liver (53.57% - 25.12%), and kidney (23.23% - 2.71%). At the same time, uptake of Tc-99m pertechnetate occurred at thyroid gland, nasal, stomach, and bladder. It is likely that stomach and bladder uptake were dominant.

At the period of 60 – 70 minutes after injection, thyroid elimination started, even in small amount. The same trend occurred in the heart and bladder. Totally excretion appeared at liver and kidney. Most patients were not performed Tc-99m uptake at 60 minutes in kidney, but a few of them showed the opposite. This is consistent to the kidney flow that works periodically. Uptake still occurred at stomach and nasal. High activity percentage in stomach performed that Tc-99m pertechnetate biodistribution pass through the gastro interstitial (GI) tract, although the radiopharmaceutical administered by bolus intravenous. From the ICRP 53 report, stated from some research showed Tc-99m pertechnetate uptake in thyroid gland, saliva gland, and stomach, also late uptake in colon (ICRP, 1987). For futher evaluation, data from Table 4.2 are shown in the form of biodistribution curve in Figure 4.1 and 4.2.

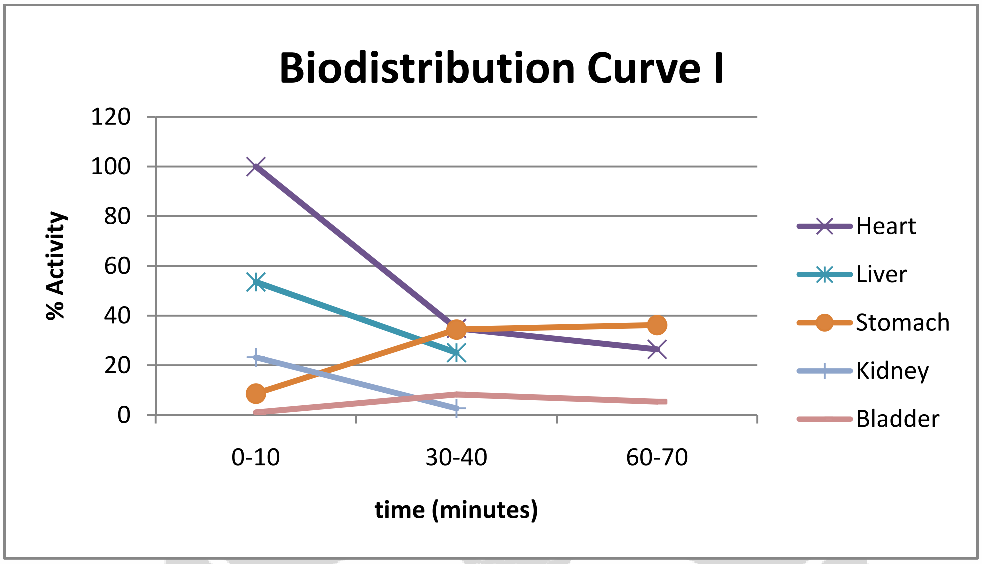

Figure 4.1 Biodistribution percentage of Tc-99m pertechnetate of heart, liver, stomach, kidney, and bladder.

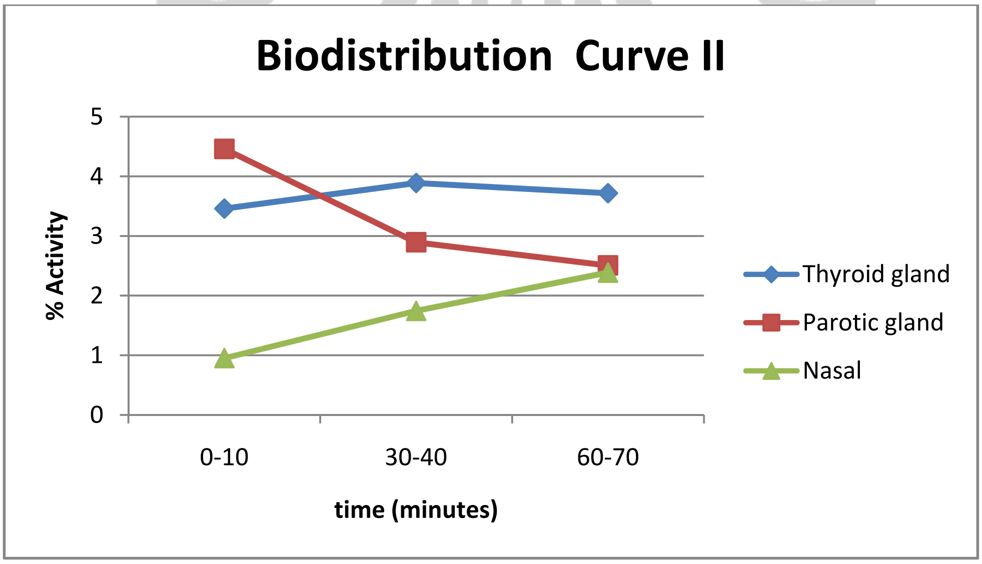

Figure 4.2 Biodistribution percentage of Tc-99m pertechnetate of thyroid gland, parotic gland, and nasal.

The curves showed all of the biodistribution percentage started to decrease at 60-70 minutes (30-40 minutes for liver and kidney), except for stomach and nasal.

Additional measurement at 90 -100 minutes for stomach is illustrated in Figure 4.3 shows that maximum biodistribution percentage occurred at period 30- 40 minutes, constant at period 60-70 minutes, and decreased at period 90-100 minutes.

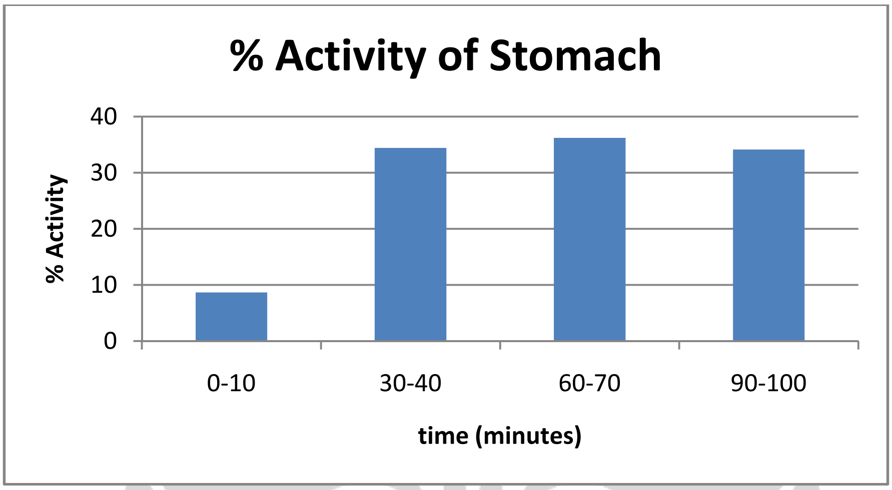

Figure 4.3 Bar diagram of stomach at the interval time

Additional measurement was also performed for nasal. The biodistribution percentage of nasal increased until 90-100 minutes as shown in Figure 4.4. This condition happened because there is not any outlet duct from nasal system to other organs, except blood vessel. Tc-99m pertechnetate would be accumulated there and it decrease slowly in biological elimination, but physics decay elimination was dominant.

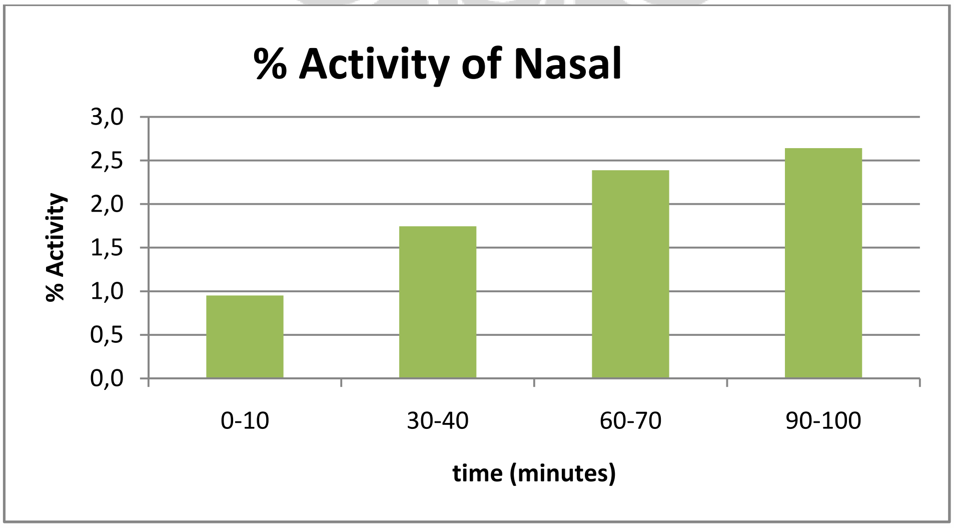

Figure 4.4 Bar diagram of nasal at the interval time

This study obtained lower activity percentage (1.30%) than Tc-99m pertechnetate biokineticks from ICRP that showed 2.67% for thyroid gland (ICRP, 1987). In this publication was not reported another measurement of activity in any organs.

This study was compared by study of Tc-99m pertechnetate biodistribution in mice (Zuicker, 2004), shown in Table 4.3.

Table 4.3 Activity percentage Tc-99m pertechnetate in Thyroid, Salivary gland, and stomach of human and mice

Time (min)	Thyroid		Salivary Gland		Stomach	
	This Study	Zuicker, 2004	This Study	Zuicker, 2004	This Study	Zuicker, 2004
0-10	1.15 ± 0.47	-	1.49 ± 0.57	-	2.88 ± 0.90	-
20	-	1.67 ± 0.40	-	2.91 ± 1.08	-	5.35 ±2.15
30-40	1.30 ± 0.25	-	0.97 ± 0.42	-	11.47 ± 2.21	-
60-70	1.24 ± 0.26	-	0.84 ± 0.38	-	12.07 ± 2.21	-
90-100	-	-	-	-	11.38 ± 2.77	-
120	-	4.76 ± 0.35	-	4.40 ± 1.07	-	15.04 ± 4.50

Table 4.4 Activity percentage Tc-99m pertechnetate in liver and kidney of human and mice

Time (min)	**Liver**		**Kidney**	
	This Study	Zuicker, 2004	This Study	Zuicker, 2004
0-10	17.85 ± 3.78	-	7.14 ± 2.27	-
20	-	0.64 ± 0.07	-	0.46 ± 0.02
30-40	8.37 ± 2.12	-	0.90 ± 0.28	-
60-70	-	-	-	-
90-100	-	-	-	-
120	-	0.66 ± 0.19	-	0.59 ± 0.04

Biodistribution of several radiopharmaceuticals included Tc-99m pertechnetate have been investigated in mice (Zuicker, 2004). From percentage point of view, there was similarity in organ uptake level between human and mice, even though differ in sampling time. It seems the maximum uptake occurred in stomach, followed by saliva gland, and thyroid.

In this study, liver and kidney uptake were monitored up to 3 minutes after injection, and the results were higher than that occurred in mice which were sampled at about 20 minutes after injection. Tc-99m pertechnetate was absorbed quickly by liver. Therefore within 20 minutes percentage uptake at these organs in mice was already very low and reached 0.64% in liver and 0.46% in kidney.

Furthermore, biodistribution data was used to determine the source organs in internal dose calculation with MIRD method, also to calculate the accumulative activity for each organ to have the internal dose data of organs.

4.1.3 Phantom Study

Thyroid response of Tc-99m petechnetate represents its metabolism function. To study this function, on clinical practice it is depend on image related to uptake and elimination process of this radiopharmaceutical. For obtaining image optimization, the study need to do repeatedly measurements that must do in human. This problem was contrary to radiation protection principle. Based on Tc-99m pertechnetate uptake and elimination of thyroid result in this study, in house Dynamic Thyroid Phantom was created to simulate thyroid metabolism of Tc-99m pertechnetate.

.

To determine the dynamic Tc-99m pertechnetate flow, it required pharmacokinetics data and in this case from 3 healthy patients (without any thyroid disease). Particular attention was given to thyroid uptake and elimination, measurement were taken in the period of 20 minutes with dynamic scanning in order to have uptake data more accurate. After 20 minutes of dynamic scanning, measurement was done at interval of 30 minutes with static scanning. Illustrated in Figure 4.5, Tc-99m pertechnetate comply with 1 compartment model. This model is similar to that stated by Stabin (Stabin M. , 1989). From these data, the decay constant was found 6.20 x 10^{-3}/minutes, the effective half life 112.19 minutes, and the 1 compartement equation as follows

$$\%A = 1{,}42e^{(6.20\times10^{-3})t} \qquad (4\text{-}1)$$

It shows that the initial uptake percentage is 1.42% with the elimination rate 6.20 x 10^{-3} per unit time (minutes).

It was noted that the effective half life of thyroid is 112.19 minutes is still in the range of that stated by ICRP 53 from 0.86 to 3.76 hours (ICRP, 1987). Further, this effective half life was used for determining debit flow of phantom elimination.

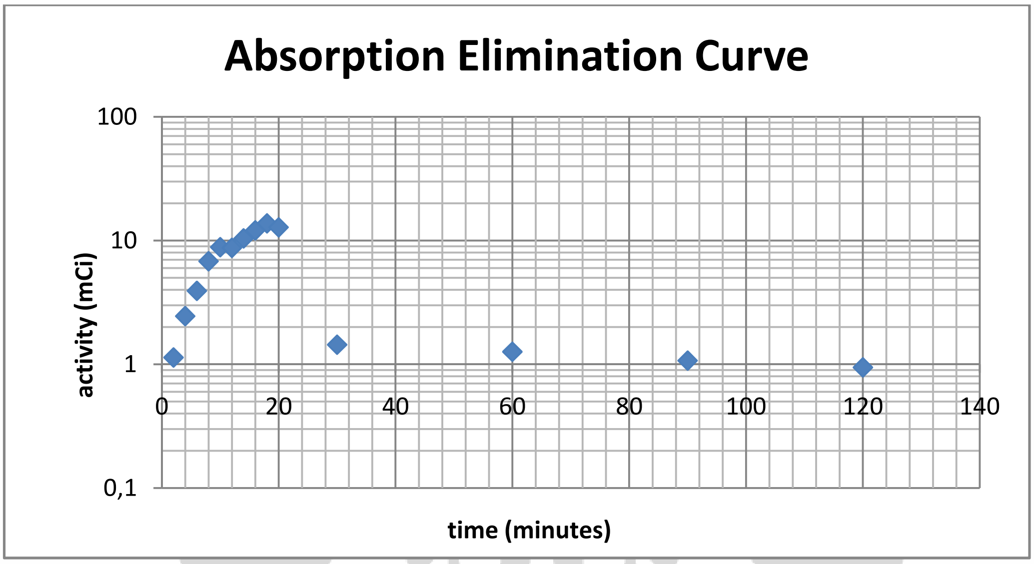

Figure 4.5 Pharmacokinetics curve of Tc-99m pertechnetate in thyroid

To verify phantom performance, five examinations with 1.96 – 2.61 mCi Tc-99m pertechnetate were done. The flow of radiopharmaceutical could be adjusted manually until the flow close similar to normal thyroid function. The result for feasibility verification contains elimination rate testing and dosimetry study for phantom. The result for elimination rate testing is shown in Table 4.5.

Table 4.5 Elimination rate and effective half life in phantom study

Measurement	***k* (/minute)**	**$T_{1/2}$ (minute)**
1	6.16E-03	112.26
2	6.15E-03	112.74
3	6.13E-03	113.05
4	6.18E-03	112.20
5	6.18E-03	112.23
Mean	6.16E-03	112.49
SD	1.95E-05	0.38

It obtained mean elimination rate 6.16 x 10^{-3}/minute and effective half life is 112.49 minutes. These results show that the phantom setting have represented Tc-99m pertechnetate elimination in thyroid, due to the result of patients measurement that obtained 6.20 x 10^{-3}/minute for elimination rate and 112.19 minutes for effective half life of Tc-99m pertechnetate in thyroid.

This phantom could also be used for dosimetry study. By count rate scanning with the same procedure at thyroid uptake patients (within 0 - 10 minutes, 30 – 40 minutes, and 60 - 70 minutes), it was found dose and dose per unit activity from thyroid dynamic phantom, as shown in Table 4.6.

Table 4.6 Dose per unit activity and effective dose equivalent (EDE) for several organs in thyroid dynamic phantom study

Measurement	$D_{rk \leftarrow rh}$ **(mGy)**	$(D_{rk \leftarrow rh})/A_0$ **(mGy/mCi)**
1	7.89E-01	3.25E-01
2	7.87E-01	3.19E-01
3	7.93E-01	3.04E-01
4	7.85E-01	3.46E-01
5	7.84E-01	4.00E-01
Mean	7.88E-01	3.39E-01
SD	3.63E-03	3.76E-02

From these measurements, it can be stated this phantom is reliable for studying thyroid uptake function.

4.1.4 Internal Dose at Several Organs

Internal dose at several organs were studied from 21 patients. All results could be seen at Appendix F. The mean dose per unit activity and Effective Dose Equivalent (EDE) were illustrated in Table 4.7.

Table 4.7 Dose per unit activity and effective dose equivalent (EDE) for several organs in patients study

Organ	Dose per unit activity $(D_{rk \leftarrow rh})/A_0$ (mGy/mCi)	EDE (H_E) (mSv/mCi)
Stomach	9.15E-02	5.49E-03
Heart	3.10E-02	1.86E-03
Liver	1.50E-02	9.00E-04
Kidney	3.33E-02	2.00E-03
Bladder	7.40E-01	4.44E-02
Thyroid	3.38E-01	1.01E-02
Total Body	1.25E+00	6.48E-02

The highest dose was received by bladder (7.40 x 10^{-1} mGy/mCi), followed by thyroid (3.38 x 10^{-1} mGy/mCi). The geometric of thyroid influenced its result of absorbed dose, since thyroid is a gland without a cavity, it contributes more of radiation than other organs with cavity, such as stomach and heart. Although thyroid had the lowest cumulative activity value from the calculation, it obtained highest dose because of the highest *S* values. Bladder as the end container of urine was the cause of high dose in bladder, moreover in this study patients were not allowed to urinate during the examination. Stomach obtained quite high dose because the retention time was high, but it has got cavity in geometrical, so the absorb dose calculation obtained the lower value than thyroid. Kidney, liver, and heart obtained low dose because of the low value of cumulative activity since time retention of Tc-99m pertechnetate in these 3 organs was very low. Cumulative activity could be seen atAppendix F. EDE per unit activity was obtained by using the weighting factor for specific tissue that given at Appendix G. For this study, EDE gave the equal values to the dose per unit activity. For further evaluation, the population of internal dose was illustrated in charts as shown in Figure 4.6 – Figure 4.11 for each organ.

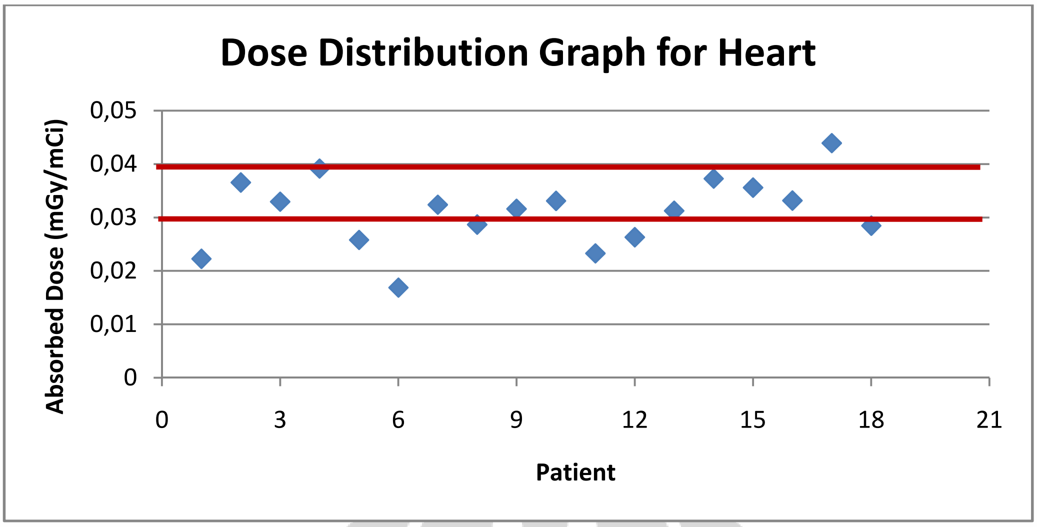

Figure 4.6 Absorb dose population of heart

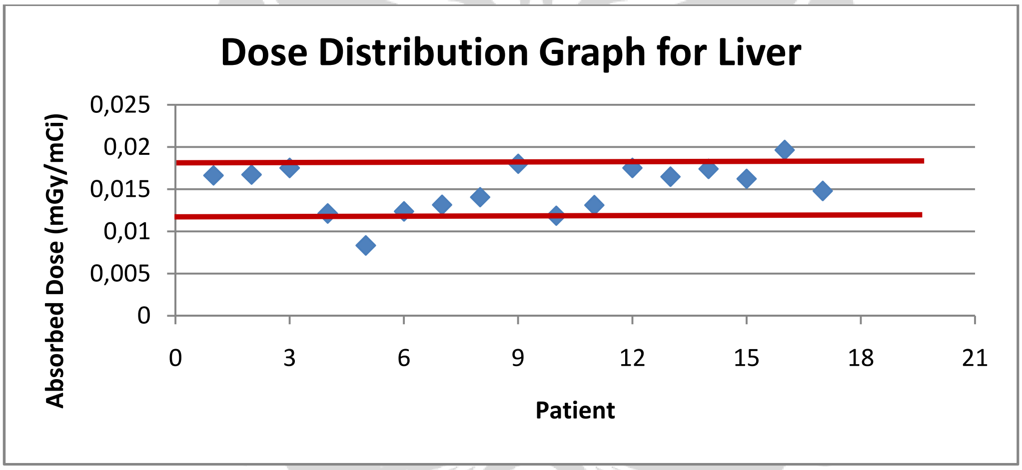

Figure 4.7 Absorb dose population of liver

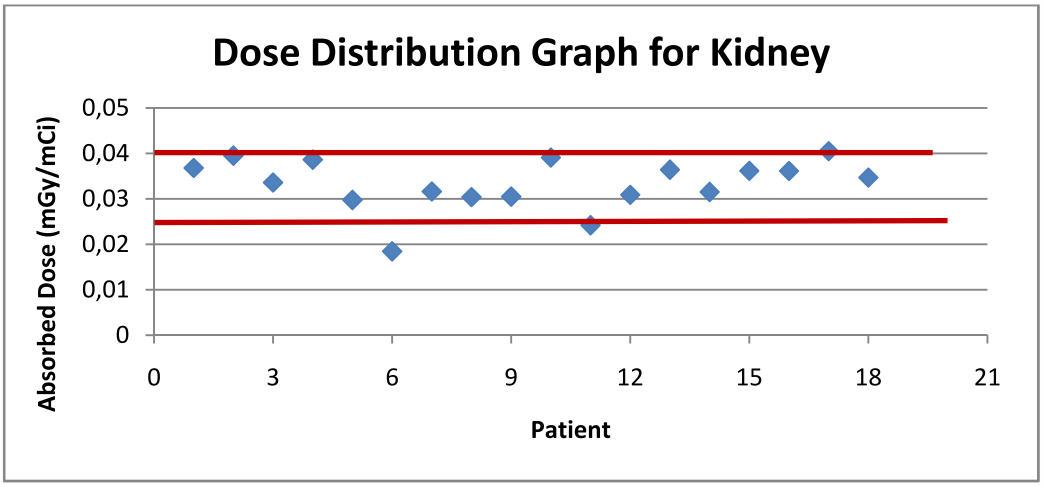

Figure 4.8 Absorb dose population of kidney

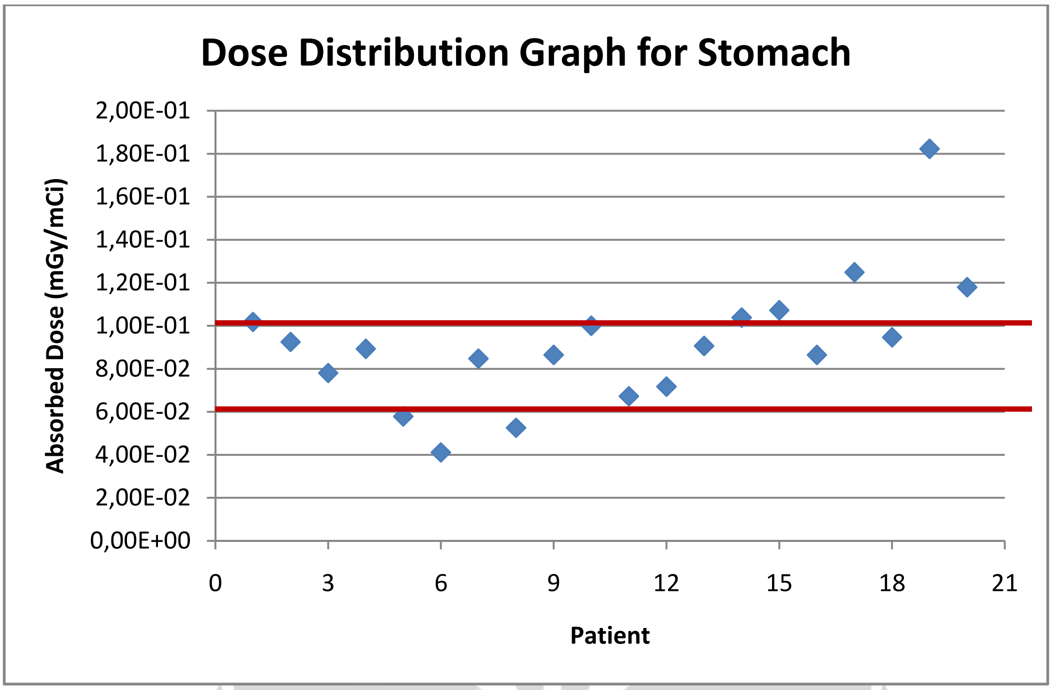

Figure 4.9 Absorb dose population of stomach

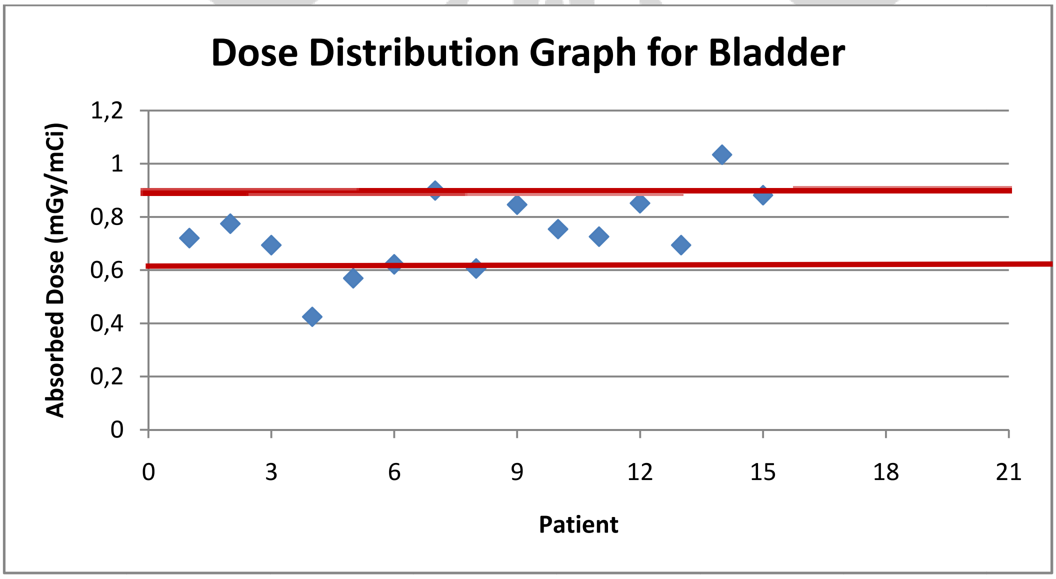

Figure 4.10 Absorb dose population of bladder

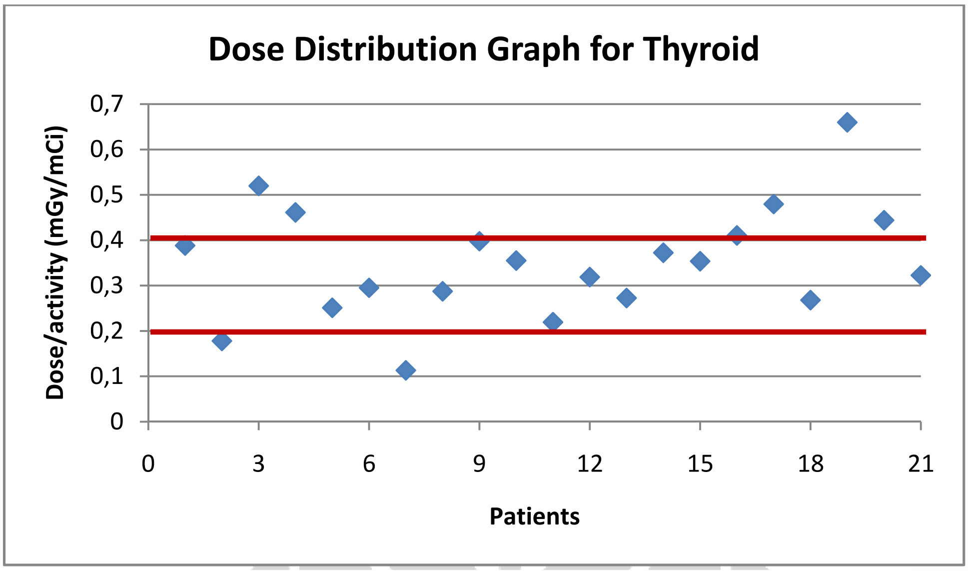

Figure 4.11 Absorb dose population for thyroid

It appears that most samples received internal absorbed dose in heart within 0.03 – 0.04 mGy/mCi (66.67%), liver within 0.012 – 0,018 mGy/mCi (88.23%), kidney 0.025 – 0.04 mGy/mCi (94.44%), stomach 0.06 – 0.1 mGy/mCi (75%), bladder 0.6 – 0.9 mGy/mCi (86.67%), and thyroid 0.2 – 0.4 mGy/mCi (71.42%). Figure 4.12 represents comparison of absorbs dose population of several organs.

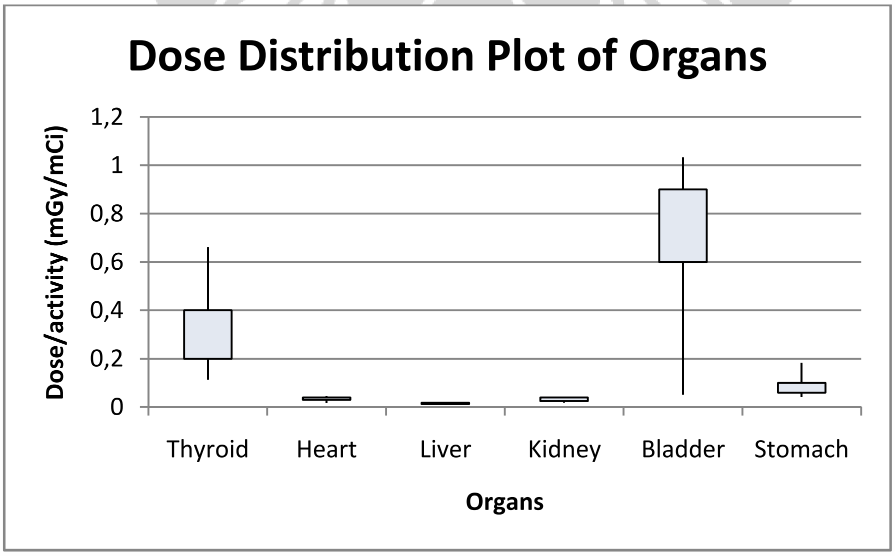

Figure 4.12 Comparison of population dose for several organs

The widest range was received by bladder, followed by thyroid. For thyroid, it was happened because the samples were patients either with healthy or unhealthy thyroid.

Most of this study results were lower than that reported by AAPM (Table 4.8), but with different distribution.

Table 4.8 Comparison dose per unit activity of this study and AAPM Report

Target Organ	**Dose per unit activity administered (mGy/mCi)**		
	This Study		AAPM (AAPM, 1992)
	Average	Range	
Thyroid	3.38×10^{-1}	$2.00 \times 10^{-1} - 4.00 \times 10^{-1}$	8.51×10^{-1}
Heart	3.10×10^{-2}	$3.00 \times 10^{-2} - 4.00 \times 10^{-2}$	1.26×10^{-1}
Liver	1.50×10^{-2}	$1.20 \times 10^{-2} - 1.80 \times 10^{-2}$	1.26×10^{-1}
Kidney	3.33×10^{-2}	$2.50 \times 10^{-2} - 4.00 \times 10^{-2}$	1.26×10^{-1}
Bladder	7.40×10^{-1}	$6.00 \times 10^{-1} - 9.00 \times 10^{-1}$	7.03×10^{-1}
Stomach	9.15×10^{-2}	$6.00 \times 10^{-2} - 1.00 \times 10^{-1}$	1.07

This study shows that bladder received the highest dose per unit activity, whereas in AAPM reports (AAPM, 1992) occurred in stomach. This difference may be due to the data in this study was collected by measurement of patient, while AAPM report were calculated by computer simulation. In fact in this study only uptake organs that could be visualized in image were observed.

If sum of internal dose in observed organs were assumed total body dose, the value of EDE for thyroid scintigraphy could be predicted. The result is 6.48×10^{-1} mSv, and the value is lower than stated by Harding, that mention effective dose of thyroid scintigraphy patient with Tc-99m is about 1,0 mSv (Harding, 2001). For comparison mean effective dose equivalent of thyroid scintigraphy with Tc-99m pertechnetate from several countries (UNSCEAR, 2008), Table 4.9 shows.

Table 4.9 Mean effective dose of Tc-99m pertechnetate for thyroid examination in some countries

Mean Effective Dose (mSv)				
This Study	Australia	Austria	Japan	Myanmar
0.65*	2,8	1,0	3,5	0,36

*Assumption: 370 MBq Tc-99m pertechnetate administered (UNSCEAR, 2008).

Consider to protection radiation problem, external dose was also done. Measurements of surface dose (SD) were also performed by using TLDs in this study. Ten patients were subjected to these measurements. The results were expressed in absorbed dose rate, shown in Table 4.10.

Table 4.10 Surface dose rate for several organs

	Dose rate/activity (mGy/mCi min)		
Patient	Thyroid	Stomach	Bladder
1	1.72E-03	1.59E-03	1.67E-03
2	2.90E-03	3.03E-03	2.90E-03
3	1.36E-03	1.52E-03	1.43E-03
4	3.93E-03	4.14E-03	4.10E-03
5	3.74E-03	2.66E-03	2.92E-03
6	3.23E-03	3.51E-03	3.08E-03
7	4.29E-03	4.37E-03	4.41E-03
8	4.17E-03	5.13E-03	4.61E-03
9	3.86E-03	4.27E-03	4.43E-03
10	4.06E-03	5.16E-03	3.63E-03
Mean	3.33E-03	3.54E-03	3.32E-03
SD	1.03E-03	1.32E-03	1.13E-03

It seems SD nearly homogenous in the anterior position, even differ in internal dose at those 3 organs. Particularly for bladder, all measurements were carried out with patients were not allowed to urinate within the measurement. Although the highest value was occurred in stomach, the values of surface dose rate were similar between those 3 organs. For further evaluation, the population data from Table 4.8 was illustrated in chart in Figure 4.13 – Figure 4.15.

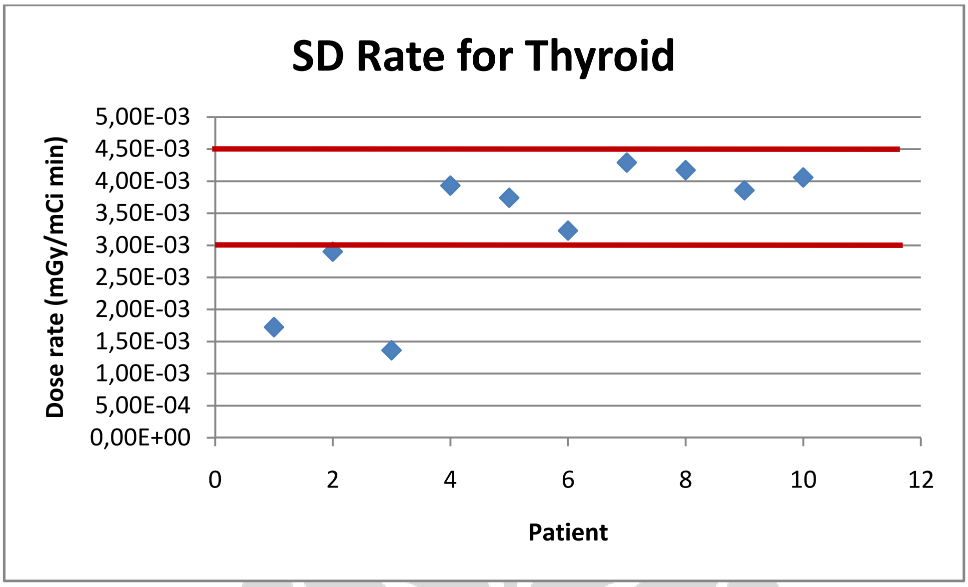

Figure 4.13 External dose rate population for thyroid

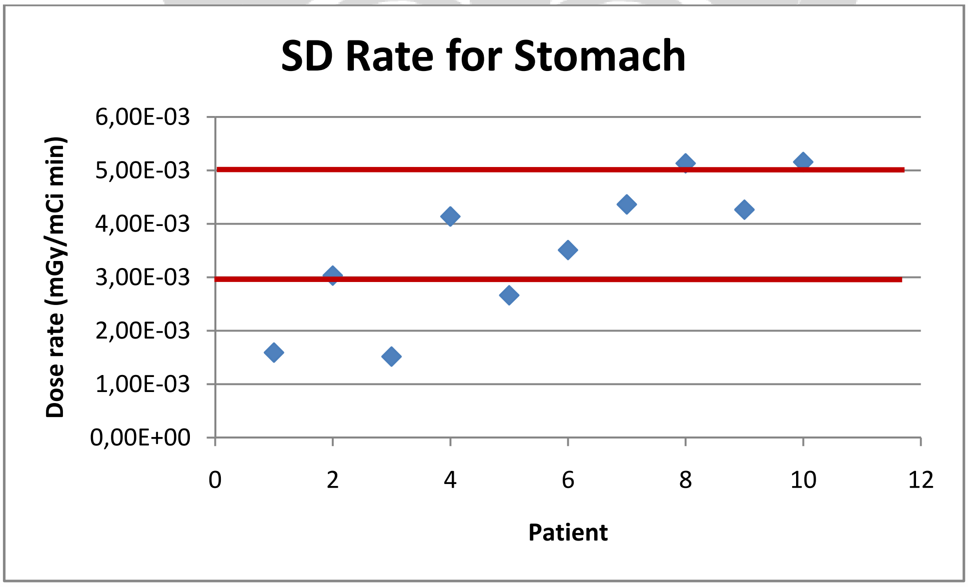

Figure 4.14 External dose rate population for stomach

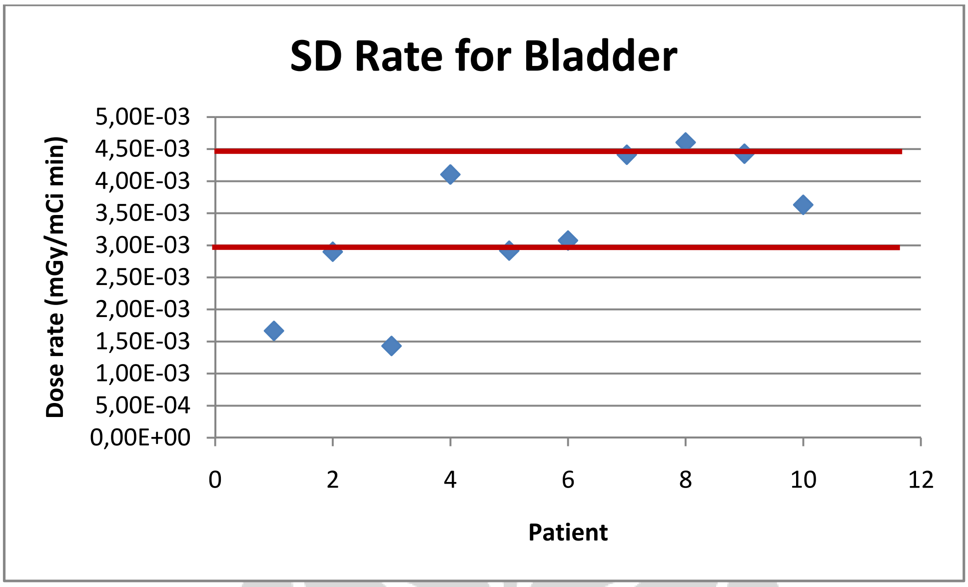

Figure 4.15 External dose rate population for bladder

The charts showed the biggest population of surface dose rate for each organ. The range of surface dose rate for thyroid is within 3.00 x 10^{-3} – 4.50 x 10^{-3} mGy/mCi min (70%), for stomach is within 3.00 x 10^{-3} – 5.00 x 10^{-3} mGy/mCi min (70%), and for bladder is within 3.00 x 10^{-3} – 4.50 x 10^{-3} mGy/mCi min (80%). Figure 4.16 represents comparison of surface dose population of these organs.

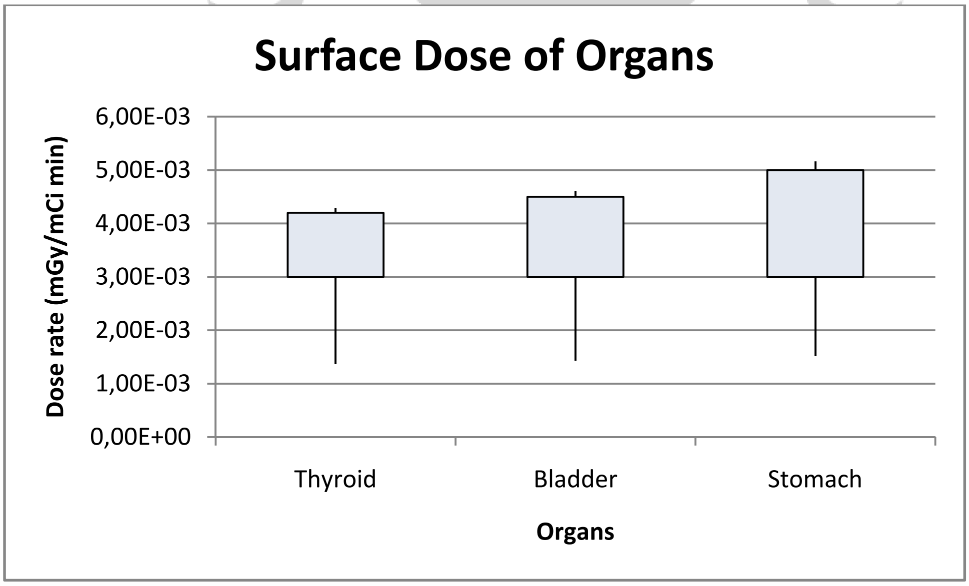

Figure 4.16 Comparison of population surface dose for several organs

4.2 Discussion

The first of this study was to obtain information about size and position that would be observed. Organs those would be observed were indicated by AP and

PA depth. The results were used for designing acrylic phantom that used for determining CCF from count per second to mCi. Since the unit in use was not SPECT-CT, it could not perform the organ size and position directly, therefore for this purpose, CT images from radiotherapy TPS were used. From this observation, it was found that the CCF did not depend on organ size by using acrylic phantom with specific organ size, compare to the phantom by using syringe in same position. Further calibration with syringe in phantom was to find count rate conversion factor (CCF).

Clinical procedure of thyroid scintigraphy in this hospital only require of scanning at a certain time. In this study, data from scanning images taken at several times which were needed, therefore special agreement was made with sample patient.Activity in organs was calculated based on count rate that displayed on ROI at scanning image and CCFs. Activity at individual organ was calculated since uptake and elimination of Tc-99m pertechnetate depend on individual metabolism, therefore it was understood that the deviation of activity for each organ is high.

Tc-99m pertechnetate was administered by bolus intravenous injection, therefore it flow directly to the heart. Uptake in the heart detected at 0 - 3 minutes. After this time, activity of Tc-99m pertechnetate in the heart fast eliminated, and the other hand liver and kidney uptake follow the heart. The longest retention occurred in stomach up to 60 – 70 minutes after injection, whereas in thyroid the retention time just only about 20 minutes. For radiation protection point of view, this information noted that location of measurement would vary with time.The measurement would be more accurate at region of heart at period 0 – 3 minutes, thyroid at period 10 – 60 minutes, and stomach at period 60 – 120 minutes. Even though in general, mean of SD almost homogenous on anterior surface. In addition, for the clinical practice, it suggests do the thyroid scanning within 15 – 20 minutes after injection because thyroid reachs the maximum uptake at this period.

Biodistribution percentage of bladder represented excretion process of Tc-99m pertechnetate in blood tract. It appears that the highest Tc-99m pertechnetate elimination was done at period 30 – 40 minutes, and decrease at 60 – 70 minutes, consistent to this radiopharmaceutical reduction in most organs.

Internal organ doses were obtained from calculation of the data activity, and indicated the highest dose per unit activity in bladder, followed by thyroid and stomach, whereas heart obtained low dose. It was different with biodistribution that the highest activity percentage was in heart. Although heart obtained 100% biodistribution percentage at the initial time, the retention time of heart is very low since the biodistribution percentage decrease from 100% at period 0-10 minutes to 34.88% at period 30-40 minutes. This condition also appeared in liver and kidney. Heart, liver, kidney obtain low dose because their low time retention, so the cumulative activity also low. In this study the dose of bladder was the highest, comparable to other organ because the patients were not allowed to urinate. But in fact, bladder dose would be lower since patient urinates frequently. Particular attention was given to internal dose of stomach. This study found value was much lower than reported by AAPM. The difference could be explained due to 2 reasons. First, in this study, measurements were carried out with time limited. Secondly, internaldose calculation in stomach did not include SI, ULI, and LLI that contribute quite high dose for stomach.

Another dose measurement was done for the surface dose (SD) by using TLDs. The homogenous result from 3 organs indicated those region occurred similar fluens rate. SD measurement supported the previously recommendation of protection radiation to consider stomach for being the reference point for patient observation. Overall, there were strong relation on biodistribution, internal dose, and SD.

To study thyroid uptake with patient would be time consuming and face several complex problems, that one of which was related to patient. Not all of patients would agree to join the study because longer times examination. Using phantom that already calibrated would be helpful. In this study, Dynamic Thyroid Phantom has been made. This phantom size is suitable to thyroid volume and position in human body. Manual adjustment of elimination flow rate could be varied, for the first it was adjusted as normal thyroid. The feasibility testing of phantom performed the elimination rate 6.16 x 10^{-3} /minute and effective half life 112.49, whereas the human study gave 6.20 x10^{-3} /minute and 112.19 minutes. It shows this phantom could simulate the thyroid elimination of Tc-99m pertechnetate. The good result was also obtained from the internal dose calculation of this phantom, i.e. 3.39 x 10^{-1} mGy/mCi, whereas in human 3.38 x 10^{-8} mGy/mCi. A verification of performance of this phantom has indicated good result. It could be used to simulate Tc-99m pertechnetate elimination as in thyroid of normal patient.

CHAPTER 5
CONCLUSION

Conclusion from this study which is related with 21 thyroid scintigraphy patients as follows

1. Human biodistribution of Tc-99m pertechnetate directly flow to heart, distribute to liver, kidney, and then flow to other organs at the period 0-10 minutes. Thyroid uptake reached maximum at period of 30-40 minutes, and stomach uptake reached the maximum at 60-70 minutes.
2. It was same with clinical practice which used administered activity of Tc-99m pertechnetate about 1.66 – 5.00 mCi, internal dose received by organs were 7.4×10^{-1} mGy/mCi for bladder, 3.38×10^{-2} mGy/mCi for thyroid, 9.15×10^{-2} mGy/mCi for stomach, 3.33×10^{-2} mGy/mCi for kidney, 3.10×10^{-2} mGy/mCi for heart, and 1.5×10^{-2} mGy/mCi for liver. Most of these values still lower than some reports.
3. Surface dose rate from TLDs measurement particularly at region of thyroid, stomach, and bladder was found respectively 3.54×10^{-3} mGy/mCi min for stomach, 3.33×10^{-3} mGy/mCi min for thyroid, and 3.32×10^{-3} mGy/mCi min for bladder.
4. For radiation protection, it was recommended measurement at period of 0 - 10 minutes in front of heart, 10 - 30 minutes in front thyroid, and 60 – 120 minutes in front of stomach.
5. Dynamic Thyroid Phantom was made in house have been passed the feasibility testing and could be used for further study to simulate Tc-99m pertechnetate in normal patient thyroid. Next study is about image optimization by comparing LEGP and pinhole collimator using for clinical and the probability to reduce number of activity administered. The limitation of this phantom is the specific in using of radiopharmaceutical and patient condition. To adjust the phantom flow, it must be calibrated first by in vivo study for each either radiopharmaceutical or patient disease that influences the thyroid metabolism.

REFERENCES

Barrall, R. C. (1992). *AAPM Task Group No. 5: Radiation Safety Consideration for The Medical Use of Technetium-99m.* New York: AAPM Publisher.

Cember, H. (1994). The biological Basis for Radiation Dosimetry. *Health Physics Society Summer School* (pp. 41-60). Wisconsin: Medical Physics Publishing.

Chiesa, C. (2010). Basic Planar Dosimetry. *Joint ICTP-IAEA School of Dosimetry Specialzing in Nuclear Medicine.* Trieste: Non.

Eckerman, K. F. (1994). Dosimetric Methodology of the ICRP. *Health Physics Society Summer School* (pp. 239-270). Wisconsin: Medical Physics Publishing.

Fisher, D. R. (1994). From Micro to Macro Internal Dosimetry. *Health Society Summer School* (pp. 61-80). Wisconsin: Health Physics Publishing.

Graham, L. S. (1991). *The SPECT Camera.* New York: AAPM Publishing.

Harding, L. K. (2001). Radiological Protection of Patients in Nuclear Medicine. *International Conference in Radiological Protection of Patients in Diagnostic and Interventional Radiology, Nuclear Medicine, and Radiotherapy* (pp. 227-233). Malaga: International Atomic Energy Agency.

ICRP 53. (1987). *Annals of The ICRP: Radiation Dose to Patients from Radiopharmaceuticals.* Oxford: Pergamon Press.

ICRP 72. (1996). *Annals of the ICRP: Age Dependent Doses to Members of the Public from Intake of Radionuclides.* Oxford: Pergamon Press.

Kereiakes, J. G., Williams, C. C., Cristy, M., & Eckerman, K. F. (1992). *AAPM Task Group No. 5: Dosimetry for Technetium-99m Labeled Pharmaceuticals.* New York: AAPM Publisher.

Lange, R. C. (1988). Basic Physics of Nuclear Medicine. In A. Gottschalk, P. B. Hoffer, & E. J. Potchen, *Diagnostic Nuclear Medicine* (p. 31). Baltimore: Williams and Wilkins.

Muehllehner, G. (1988). The Anger Scintillation Camera. In A. Gottschalk, P. B. Hoffer, & E. J. Potchen, *Diagnostic Nuclear Medicine* (p. 71). Baltimore: Williams and Wilkins.

Oppenheim, B., & Beck, R. N. (1988). The Scintillation Detector. In A. Gottschalk, P. B. Hoffer, & E. J. Potchen, *Diagnostic Nuclear Medicine* (p. 55). Baltimore: Williams and Wilkins.

Raabe, O. (1994). Introduction to Internal Radiation Dosimetry. *Health Physics Summer School* (pp. 1-26). Wisconsin: Medical Physics Publishing.

Saber, R., Wagih, S., Sedik, A., & Fawzy, A. (2001). Evaluation of Solitary Thyroid Cold Nodules with Technetium 99m Sestamibi and Thallium 201. *Journal of Egyptian National Cancer Inst. Vol. 13* , 147-155.

Sarkar, S. D., InVivo Thyroid Studies (1988). *Diagnostic Nuclear Medicine* (pp. 756). Baltimore: Williams and Wilkins.

Scanlon, V. C., & Sanders, T. (2007). *Essential of Anatomy and Physiology*. Philadelphia: Davis Company.

Shargel, L., & Yu, A. B. (2005). *Biofarmasetika dan Farmakokinetika Terapan (*Transleted from: *Applied Biopharmaceutics and Pharmacokinetics, 1985)* . Surabaya: Airlangga Press.

Simsons, G. H. (1992). *AAPM Task Group No. 5: Instrumentation in the Medical Use of Technetium-99m.* New York: AAPM Publisher.

Snyder, W. S., Ford, M. R., Warner, G. G., & Watson, S. B. (1975). "S," Absorbed Dose Per Unit Cumulated Activity for Selected Radionuclides and Organs. *Journal of Nuclear Medicine* , Pamphlet No.11.

Stabin, M. (1989). Fundamentals of Radionuclide Dosimetry. *American Association of Physicists in Medicine Summer School: Expanding the Role of Medical Physics in Nuclear Medicine* (pp. 78-95). Birmingham: American Institute of Physics.

Stabin, M. G. (1996). MIRDOSE: Personal Computer Software for Internal Dose Assessment in Nuclear Medicine. *Journal of Nuclear Medicine Voulme 37* , 538-546.

Trueblood, J. H. (1991). New Radiation Dose Limit Standards. *American Association of Physicists in Medicine Summer School: Expanding the Role of Medical Physics in Nuclear*

Ulloa, M. F. (1992). *AAPM Task Group No. 5: Clinical Application of Technetium-99m Labeled Pharmaceuticals.* New York: AAPM Publishing.

UNSCEAR. (2008). *Sources and Effects of Ionizing Radiation.* New York: UNSCEAR.

Williams, C. C. (1992). *AAPM Task Group No. 5: Production and Quality Control oc Technetium-99m Labeled Pharmaceuticals.* New York: AAPM Publishing.

Yokoyama, N., & al, e. (1986). Determination of The Voule of The Thyroid Gland by A High Resolutional Ultrasonic Scanner. *Journal of Nuclear Medicine* , 1475-1479.

Zuckier, M. L. (2004). Kineticks of Perrhenate. *Journal of Nuclear Medicine* , 500-507.

Appendix A: Organ Size and Position from CT Images Observed

Information:

a: cranial – caudally

b: lateral medial lateral

c : width

d : depth from surface to organ at AP position

e : depth from surface to organ at PA position

Particularly for liver: e: the shortest cranial caudally; f: the longest cranial caudally

Unit: centi meter (cm)

Table 1 Approximation of heart size and position

Patient	Coronal				Sagital					Axial					
	a	b	c	SD	a	c	d	e	SD	a	b	c	d	e	SD
1	11.371	12.590	4.560	0.109	10.288	8.960	2.549	6.797	0.109	9.900	8.530	8.314	2.365	7.627	0.108
2	11.125	12.688	6.888	0.187	9.265	7.269	2.907	6.476	0.187	10.500	8.470	7.329	2.388	7.082	0.116
3	8.763	10.735	7.884	0.094	9.214	7.933	4.067	8.200	0.094	7.200	8.734	7.486	3.854	7.637	0.105
4	10.999	9.782	7.070	0.095	10.554	8.174	3.281	8.437	0,095	10.500	8.459	7.694	2.824	8.683	0.100
5	10.976	10.610	7.560	0.165	10.625	7.462	2.565	7.812	0.165	10.200	7.753	7.623	2.966	7.623	0.100
6	8.499	12.511	8.288	0.169	8.140	9.443	3.108	6.933	0.169	7.350	12.574	8.420	3.204	6.410	0.105
7	11.987	12.663	9.310	0.245	12.867	9.367	3.469	10.755	0.245	9.600	12.630	9.412	2.745	9.902	0.139
8	9.301	10.311	9.500	0.111	12.218	8.815	3.070	9.130	0.111	5.016	10.101	8.153	2.340	9.059	0.107
9	9.863	11.511	7.626	0.172	7.793	8.511	4.012	7.781	0.172	7.050	8.717	8.064	2.827	7.981	0.118
10	9.197	10.316	6.786	0.161	9.196	8.049	3.061	7.142	0.161	6.900	8.380	7.137	2.275	6.980	0.111
11	12.070	12.222	10.212	0.120	-	6.535	2.376	8.840	0.120	12.000	7.475	6.596	2.149	8.079	0.105
12	9.095	9.591	8.436	0.120	8.500	8.318	1.698	6.281	0.120	6.600	9.292	7.551	2.517	7.170	0.108
13	12.101	11.040	10.004	0.123	9.751	7.474	3.912	9.041	0.123	7.800	10.608	10.623	4.365	8.812	0.116
14	13.666	10.661	8.890	0.101	9.751	8.529	4.122	8.458	0.101	8.850	10.784	8.683	3.601	8.329	0.100
15	12.229	12.952	8.586	0.087	12.724	5.797	4.132	9.683	0.087	11.550	-	-	2.529	7.586	0.115
16	11.205	12.836	8.658	0.167	9.789	8.715	3.651	8.361	0.167	9.600	11.879	8.358	2.787	8.433	0.106
17	10.515	9.859	7.225	0.181	9.489	8.963	4.225	7.683	0.181	8.700	9.368	9.468	3.328	8.018	0.121
18	12.493	11.885	11.165	0.119	10.805	10.199	4.214	8.682	0.119	11.550	6.370	5.457	7.609	8.762	0.109
19	14.768	11.874	9.163	0.110	-	10.562	3.984	7.656	0.110	12.750	11.137	-	3.950	7.590	0.109
20	10.681	12.877	8.778	0.112	8.703	9.243	2.528	8.848	0.112	8.250	9.565	9.039	2.781	8.962	0.109

Table 2 Approximation of liver size and position (Continued)

Patient	Coronal				Sagital					Axial						
	a	b	c	SD	a	c	d	e	SD	a	b	c	d	e	f	SD
1	15.548	21.163	12.236	0.109	12.067	11.974	2.085	2.626	0.109	14.400	19.193	13.043	2.365	2.670	13.653	0.108
2	16.544	19.824	13.202	0.187	10.324	11.102	1.718	3.040	0.187	18.300	19.736	13.671	1.976	1.896	14.165	0.116
3	14.688	20.831	11.470	0.094	8.880	11.317	3.667	5.537	0.094	13.350	19.539	13.930	3.261	3.484	14.528	0.105
4	12.370	17.140	13.440	0.165	-	7.695	3.148	8.511	0.165	15.000	17.198	12.847	2.965	2.188	14.541	0.100
5	14.365	20.201	13.764	0.169	9.936	12.551	2.032	3.825	0.169	17.850	13.710	20.088	2.013	2.310	15.796	0.105
6	15.636	21.684	14.896	0.245	8.860	13.714	3.474	4.684	0.245	15.200	21.355	16.176	3.727	3.629	17.941	0.139
7	10.247	17.631	15.225	0.111	-	-	1.968	2.833	0.111	11.850	17.941	14.872	2.869	2.944	17.516	0.107
8	17.047	20.183	11.537	0.172	-	-	3.891	7.661	0.172	17.100	19.674	11.140	4.240	2.910	13.053	0.118
9	15.554	20.179	12.090	0.161	9.991	10.769	2.834	5.101	0.161	17.250	17.856	12.784	2.980	1.961	13.725	0.111
10	13.260	21.051	16.200	0.120	-	-	2.971	-	0.120	-	20.964	14.083	3.039	3.632	13.045	0.105
11	18.445	21.983	12.996	0.120	13.125	11.889	1.443	2.971	0.120	16.350	19.574	14.035	2.059	0.915	8.619	0.108
12	16.803	17.560	15.744	0.123	-	-	3.043	5.303	0.123	15.600	15.624	14.824	3.541	5.435	18.447	0.116
13	13.382	17.562	13.580	0.101	-	-	-	-	-	11.550	12.969	17.365	2.329	1.341	16.165	0.100
14	13.448	20.332	13.800	0.134	-	-	2.175	9.646	0.134	13.950	-	-	1.874	1.455	13.049	0.098
15	10.379	17.311	13.425	0.167	10.143	13.190	3.297	3.062	0.167	13.350	16.014	14.080	2.560	3.388	14.457	0.106
16	12.567	19.847	19.376	0.181	8.976	14.100	3.457	4.738	0.181	14.700	18.652	15.182	3.156	2.559	11.856	0.121
17	19.330	18.460	-	0.119	13.422	14.919	3.540	4.720	0.119	19.200	16.808	-	3.536	4.612	16.141	0.109
18	17.055	22.576	13.398	0.110	-	12.499	2.666	4.062	0.110	16.350	21.577	-	3.099	3.098	13.710	0.109
19	18.909	23.068	13.604	0.112	-	-	-	-	-	16.350	21.059	13.674	2.395	4.249	12.593	0.109
20	11.500	20.226	14.118	0.163	-	-	2.298	3.333	0.163	12.300	19.535	-	2.286	2.838	13.242	0.111

(Continued)

Table 3 Approximation of kidney size and position

Patient	Coronal				Sagital					Axial					
	a	b	c	SD	a	c	d	e	SD	a	b	c	d	e	SD
1	10.509	4.430	4.970	0.165	10.042	4.780	10.027	4.197	0.165	9.450	4.581	4.871	10.306	3.741	0.100
2	10.534	5.618	10.168	0.169	9.336	4.184	11.236	3.944	0.169	10.800	4.545	4.390	9.761	3.055	0.105
3	10.597	5.725	5.664	0.246	10.078	4.684	11.796	5.551	0.245	10.000	6.069	4.902	12.843	5.490	0.139
4	6.779	6.611	5.092	0.111	6.858	5.037	12.672	3.148	0.111	9.450	6.558	5.133	12.683	3.473	0.107
5	10.715	6.079	4.897	0.172	10.715	4.985	10.213	3.404	0.172	10.650	5.728	4.905	10.475	3.409	0.118
6	11.240	4.875	9.360	0.160	10.785	4.875	10.316	3.401	0.161	10.050	4.307	4.471	10.510	3.137	0.111
7	10.370	4.753	4.440	0.120	10.200	4.414	12.307	4.074	0.120	9.900	5.225	4.470	11.785	3.854	0.105
8	10.880	6.281	5.320	0.120	11.135	4.244	10.440	1.952	0.120	10.950	1.831	4.951	8.543	1.831	0.108
9	10.838	6.557	4.466	0.112	10.127	4.266	12.794	4.898	0.112	11.550	5.099	6.788	11.897	4.867	0.109
10	8.967	5.390	5.494	0.123	8.271	4.260	13.561	5.824	0.123	9.150	5.098	4.941	14.000	5.024	0.116
11	8.185	4.478	4.970	0.101	7.402	4.264	7.463	4.052	0.101	6.600	4.934	4.659	7.059	3.247	0.100
12	11.204	6.124	4.725	0.167	10.733	4.593	11.070	4.956	0.167	10.350	5.939	4.292	11.294	4.969	0.106
13	10.131	6.402	5.270	0.181	9.874	4.610	11.396	4.866	0.181	9.600	5.536	5.374	10.321	4.691	0.120
14	10.890	5.816	5.016	0.119	9.876	5.142	11.885	4.130	0.119	10.650	5.603	4.996	12.452	3.766	0.109
15	10.568	5.279	4.864	0.106	9.318	4.135	11.578	3.759	0.106	9.300	-	-	11.194	4.523	0.108
16	-	-	5.688	0.107	9.826	5.661	11.850	4.679	0.107	-	-	-	-	-	-
17	11.530	5.769	5.460	0.194	10.607	4.257	11.915	2.648	0.314	9.000	-	-	5.762	3.262	0.098
18	9.775	6.091	6.320	0.163	9.085	5.861	9.768	4.252	0.163	9.600	6.223		10.011	5.754	0.111
19	10.365	5.407	4.560	0.109	10.210	3.939	10.273	3.321	0.109	9.750	4.804	4.501	8.467	3.051	0.108
20	10.986	4.758	4.182	0.187	10.456	4.493	10.705	3.172	0.187	10.500	4.358	3.871	10.541	2.801	0.116

(Continued)

Table 4 Approximation of bladder size and position

Patient	Coronal				Sagital					Axial					
	a	b	c	SD	a	c	d	e	SD	a	b	c	d	e	SD
1	11.236	7.422	8.140	0.169	5.985	8.487	2.271	7.172	0.169	6.900	10.490	7.675	2.384	7.526	0.105
2	7.444	9.485	7.350	0.092	7.509	5.281	4.694	12.844	0.092	7.950	9.496	-	4.510	12.745	0.092
3	5.504	9.277	6.764	0.084	5.799	7.209	5.850	9.573	0.084	5.100	9.710	-	5.889	9.368	0.084
4	8.513	9.327	9.492	0.083	9.661	8.068	3.011	7.105	0.170	8.850	9.637	-	3.021	9.637	0.119
5	4.670	8.637	5.680	0.075	7.181	5.246	4.133	8.161	0.075	2.25	7.351	4.080	4.960	11.921	0.113
6	7.279	10.902	7.770	0.112	10.443	7.031	2.370	7.548	0.112	9.600	10.555	6.855	2.012	7.749	0.105
7	8.075	10.286	11.470	0.073	8.051	8.063	4.910	5.737	0.073	14.400	-	-	4.024	4.173	0.105
8	6.618	7.798	5.002	0.187	5.956	6.092	3.040	7.533	0.187	5.700	7.895	5.353	2.719	7.741	0.116
9	5.684	9.327	7.326	0.070	5.573	5.527	16.088	8.044	0.070	8.100	-	-	3.502	8.718	0.105
10	4.988	6.724	4.290	0.088	7.109	4.420	3.673	9.962	0.088	6.600	6.187	3.687	3.373	10.588	0.111
11	7.331	8.349	9.348	0.086	8.240	8.713	5.929	7.683	0.175	5.400	-	-	5.465	8.565	0.115
12	4.066	8.571	7.546	0.106	5.320	4.812	4.060	9.699	0.106	3.450	-	-	3.603	11.270	0.108
13	3.383	7.569	3.375	0.088	7.704	6.568	20.956	6.756	0.089	11.250	-	-	9.939	6.626	0.106
14	3.905	6.755	3.420	0.078	3.135	4.668	4.558	10.544	0.078	3.600	6.735	4.157	4.549	10.745	0.111
15	5.051	10.460	7.298	-	4.427	6.973	4.421	9.215	0.088	5.100	10.937	-	4.776	10.212	0.116
16	6.630	9.457	6.650	-	-	-	3.688	4.257	0.134	4.350	9.495	-	2.152	10.829	0.098
17	4.384	5.887	4.108	0.107	2.797	6.642	7.698	5.132	0.107	-	-	-	-	-	-
18	6.387	10.194	7.881	0.074	6.701	8.468	3.502	7.005	0.074	6.900	8.718	6.743	4.188	7.808	0.100
19	5.842	7.965	4.836	0.079	4.550	4.431	5.161	10.153	0.079	4.800	7.754	-	4.863	10.275	0.111
20	7.590	8.504	7.533	0.163	-	-	4.597	8.159	0.163	6.150	8.034	-	4.414	7.488	0.111

(Continued)

Table 5 Approximation of stomach position

Patient	Axial		
	d	e	SD
1	13.271	3.600	0.100
2	6.266	3.335	0.105
3	10.588	4.235	0.100
4	13.787	5.603	1.105
5	8.589	4.521	0.105
6	8.762	4.689	0.109
7	8.752	3.330	0.110
8	8.946	3.143	0.114
9	7.258	2.107	0.110
10	8.942	4.620	0.105
11	8.163	3.360	0.113
12	8.140	4.033	0.103
13	6.534	3.755	0.106
14	8.918	4.617	0.113
15	8.914	4.869	0.106

Table 6 AP and PA depth of organs

Organ	For Calibration	
	AP	PA
Heart	3.12 ± 0.61	8.06 ± 0.95
Liver	2.76 ± 0.74	3.80 ± 0.93
Kidney	11.04 ± 1.21	3.97 ± 0.96
Bladder	4.18 ± 0.99	8.61 ± 1.34
Stomach	9.06 ± 2.10	3.99 ± 0.88

Appendix B: Count Rate Conversion Factor (CCF)

<u>Information</u>

The value of count rate was obtained as follow:

t was counting time = 180 seconds

$$\text{Count rate} = \frac{(counts - background)}{t}$$

Table 1 CCF measurement of thyroid

Activity			Mean	Count rate AP (cps)			Mean	Count rate PA (cps)			Mean	Mean activity/count rate (mCi/cps)	
1	2	3		1	2	3		1	2	3		AP	PA
1.05E+00	1.02E+00	1.01E+00	1.03E+00	4.39E+03	4.34E+03	4.33E+03	4.35E+03	1.08E+03	1.07E+03	1.06E+03	1.07E+03	2.36E-04	9.61E-04
2.02E+00	2.01E+00	1.96E+00	2.00E+00	8.39E+03	8.33E+03	8.28E+03	8.33E+03	2.06E+03	2.06E+03	2.09E+03	2.07E+03	2.40E-04	9.64E-04
3.01E+00	3.00E+00	2.98E+00	3.00E+00	1.34E+04	1.33E+04	1.31E+04	1.33E+04	3.28E+03	3.27E+03	3.25E+03	3.27E+03	2.26E-04	9.17E-04
4.03E+00	4.02E+00	3.96E+00	4.00E+00	1.72E+04	1.71E+04	1.69E+04	1.71E+04	4.24E+03	4.23E+03	4.19E+03	4.22E+03	2.34E-04	9.48E-04
5.02E+00	5.01E+00	4.96E+00	5.00E+00	2.04E+04	2.03E+04	2.02E+04	2.03E+04	5.10E+03	5.06E+03	5.02E+03	5.06E+03	2.46E-04	9.88E-04
											Mean	2.36E-04	9.56E-04
											SD	7.31E-06	2.59E-05

Table 2 CCF measurement of heart

Activity			Mean	Count rate AP (cps)			Mean	Count rate PA (cps)			Mean	Mean activity/count rate (mCi/cps)	
1	2	3		1	2	3		1	2	3		AP	PA
1.08E+00	1.07E+00	1.06E+00	1.07E+00	2.94E+03	2.92E+03	2.98E+03	2.95E+03	1.49E+03	1.48E+03	1.15E+03	1.37E+03	3.63E-04	7.80E-04
2.02E+00	2.00E+00	1.98E+00	2.00E+00	5.41E+03	5.37E+03	4.94E+03	5.24E+03	2.64E+03	2.63E+03	2.46E+03	2.58E+03	3.82E-04	7.76E-04
3.01E+00	3.00E+00	2.95E+00	2.99E+00	8.00E+03	7.89E+03	7.39E+03	7.76E+03	3.21E+03	3.20E+03	3.58E+03	3.33E+03	3.85E-04	8.97E-04
4.04E+00	4.02E+00	3.98E+00	4.01E+00	1.07E+04	1.07E+04	1.07E+04	1.07E+04	4.39E+03	4.37E+03	4.25E+03	4.34E+03	3.75E-04	9.26E-04
5.04E+00	5.00E+00	4.96E+00	5.00E+00	1.40E+04	1.39E+04	1.41E+04	1.40E+04	5.47E+03	5.43E+03	5.30E+03	5.40E+03	3.57E-04	9.26E-04
											Mean	3.72E-04	8.61E-04
											SD	1.19E-05	7.66E-05

(Continued)

Table 3 CCF measurement of liver

Activity			Mean	Count rate AP (cps)			Mean	Count rate PA (cps)			Mean	Mean activity/count rate (mCi/cps)	
1	2	3		1	2	3		1	2	3		AP	PA
1.04E+00	1.02E+00	1.01E+00	1.02E+00	4.05E+03	4.02E+03	4.06E+03	4.04E+03	2.69E+03	2.68E+03	2.69E+03	2.69E+03	2.53E-04	3.81E-04
2.02E+00	2.01E+00	1.96E+00	2.00E+00	7.50E+03	7.44E+03	7.44E+03	7.46E+03	4.99E+03	4.96E+03	4.94E+03	4.96E+03	2.68E-04	4.02E-04
3.01E+00	3.00E+00	2.98E+00	3.00E+00	1.14E+04	1.13E+04	1.14E+04	1.14E+04	7.50E+03	7.44E+03	7.39E+03	7.44E+03	2.64E-04	4.03E-04
4.03E+00	4.02E+00	3.96E+00	4.00E+00	1.49E+04	1.48E+04	1.48E+04	1.48E+04	9.83E+03	9.78E+03	9.72E+03	9.78E+03	2.70E-04	4.09E-04
5.02E+00	5.01E+00	4.96E+00	5.00E+00	1.82E+04	1.81E+04	1.79E+04	1.81E+04	1.21E+04	1.19E+04	1.19E+04	1.20E+04	2.76E-04	4.18E-04
											Mean	2.66E-04	4.02E-04
											SD	8.67E-06	1.38E-05

Table 4 CCF measurement of kidney

Activity			Mean	Count rate AP (cps)			Mean	Count rate PA (cps)			Mean	Mean activity/count rate (mCi/cps)	
1	2	3		1	2	3		1	2	3		AP	PA
1.06E+00	1.05E+00	1.04E+00	1.05E+00	1.57E+03	1.52E+03	1.49E+03	1.53E+03	2.64E+03	2.62E+03	2.60E+03	2.62E+03	6.86E-04	4.00E-04
2.06E+00	2.06E+00	2.02E+00	2.05E+00	2.95E+03	2.92E+03	2.87E+03	2.91E+03	5.05E+03	5.01E+03	4.89E+03	4.98E+03	7.03E-04	4.11E-04
3.01E+00	2.99E+00	2.96E+00	2.99E+00	4.26E+03	4.21E+03	4.19E+03	4.22E+03	7.22E+03	7.11E+03	7.06E+03	7.13E+03	7.07E-04	4.19E-04
4.09E+00	4.05E+00	4.02E+00	4.05E+00	5.78E+03	5.72E+03	5.67E+03	5.72E+03	9.56E+03	9.56E+03	9.44E+03	9.52E+03	7.08E-04	4.26E-04
5.07E+00	5.01E+00	4.99E+00	5.02E+00	7.17E+03	7.11E+03	7.06E+03	7.11E+03	1.18E+04	1.17E+04	1.16E+04	1.17E+04	7.06E-04	4.29E-04
											Mean	7.02E-04	4.17E-04
											SD	9.31E-06	1.18E-05

(Continued)

Table 5 CCF measurement of bladder

Activity			Mean	Count rate AP (cps)			Mean	Count rate PA (cps)			Mean	Mean activity/count rate (mCi/cps)	
1	2	3		1	2	3		1	2	3		AP	PA
1.05E+00	1.45E+00	1.04E+00	1.18E+00	3.16E+03	3.14E+03	3.11E+03	3.14E+03	1.41E+03	1.40E+03	1.39E+03	1.40E+03	3.76E-04	8.44E-04
2.09E+00	2.08E+00	2.07E+00	2.08E+00	6.11E+03	6.11E+03	6.00E+03	6.07E+03	2.76E+03	2.73E+03	0.00E+00	1.83E+03	3.42E-04	1.14E-03
3.06E+00	3.03E+00	3.01E+00	3.03E+00	8.78E+03	8.72E+03	8.67E+03	8.72E+03	3.96E+03	3.92E+03	3.91E+03	3.93E+03	3.48E-04	7.73E-04
4.07E+00	4.04E+00	4.01E+00	4.04E+00	1.16E+04	1.15E+04	1.13E+04	1.15E+04	5.22E+03	5.19E+03	5.15E+03	5.19E+03	3.52E-04	7.79E-04
5.06E+00	4.99E+00	4.94E+00	5.00E+00	1.41E+04	1.41E+04	1.39E+04	1.40E+04	6.44E+03	6.39E+03	6.33E+03	6.39E+03	3.56E-04	7.82E-04
											Mean	3.55E-04	8.63E-04
											SD	1.30E-05	1.56E-04

Table 6 CCF measurement of stomach

Activity		Mean	Count rate AP (cps)		Mean	Count rate PA (cps)		Mean	Mean activity/count rate (mCi/cps)	
1	2		1	2		1	2		AP	PA
1.05E+00	1.45E+00	1.25E+00	2.08E+03	2.07E+03	2.07E+03	2.69E+03	2.68E+03	2.69E+03	6.03E-04	4.65E-04
2.04E+00	2.08E+00	2.06E+00	3.64E+03	3.62E+03	3.63E+03	4.72E+03	4.67E+03	4.69E+03	5.68E-04	4.39E-04
3.06E+00	3.03E+00	3.05E+00	5.49E+03	5.44E+03	5.47E+03	7.11E+03	7.06E+03	7.08E+03	5.57E-04	4.30E-04
4.07E+00	4.04E+00	4.06E+00	7.33E+03	7.28E+03	7.31E+03	9.39E+03	9.33E+03	9.36E+03	5.55E-04	4.33E-04
5.06E+00	4.99E+00	5.03E+00	9.00E+03	8.94E+03	8.97E+03	1.14E+04	1.14E+04	1.14E+04	5.60E-04	4.40E-04
								Mean	5.69E-04	4.41E-04
								SD	1.99E-05	1.40E-05

Appendix C: Patient Data in This Study

Patient	Gender	Age (years old)	Comment	A_o(mCi)
1	Female	37	Struma nodusa	3.298
2	Female	54	Thyroiditis	2.92
3	Male	31	Nodule	2.454
4	Female	53	Struma nodusa	3.074
5	Female	57	Struma nodusa	4.479
6	Male	34	Nodule	5
7	Female	48	Nodule	4.071
8	Female	41	Nodule	4.161
9	Female	31	Nodule	3.926
10	Male	24	Normal	2.46
11	Male	25	Normal	3.666
12	Female	23	Nodule	3.999
13	Male	27	Normal	2.504
14	Female	19	Normal	2.973
15	Female	53	Normal	2.923
16	Female	29	Nodule	2.983
17	Female	26	Normal	2.7
18	Male	22	Normal	2.846
19	Female	21	Normal	1.66
20	Female	18	Normal	2.678
21	Male	28	Hot Nodule	2.588

Appendix D: Count Rate and Activity Percentage of Organs

Information

Activity: $A = \sqrt{(I_{AP} \times CCF_{AP})(I_{PA} \times CCF_{PA})}$ Activity Percentage: $\%A = A_t / A_0$

Table 1 Count rate of thyroid from image scanning at the interval time

Patient	Time (minute)			Time (minute)			Time (minute)			Time (minute)		
	0-10		Activity	30-40		Activity	60-70		Activity	90-100		Activity
	AP	PA	(mCi)	AP	PA	(mCi)	AP	PA	(mCi)			(mCi)
1	17472	11943	3.90E-02	172208	16089	1.46E-01	39242	10930	5.73E-02	-	-	-
2	12969	3785	1.09E-02	5921	2010	9.54E-03	1861	1236	4.19E-03	-	-	-
3	321019	147387	5.31E-01	346142	222799	7.68E-01	463078	99614	5.94E-01	-	-	-
4	37862	17643	7.13E-02	36088	15925	6.63E-02	33503	14360	6.07E-02	-	-	-
5	25194	10928	3.19E-02	13983	5200	2.36E-02	15481	5791	2.62E-02	-	-	-
6	332726	225424	2.00E+00	1685641	399107	2.27E+00	1367057	251312	1.62E+00	-	-	-
7	3054	1656	5.03E-03	2441	1184	4.70E-03	2107	860	3.72E-03	-	-	-
8	29121	13891	4.12E-02	31016	9877	4.84E-02	26784	9778	4.48E-02	-	-	-
9	76076	35182	1.10E-01	71140	20016	1.04E-01	55487	19880	9.19E-02	-	-	-
10	57730	29061	9.04E-02	42832	13461	6.64E-02	32366	11328	5.30E-02	-	-	-
11	40368	22858	5.21E-02	30269	11019	5.05E-02	22843	8480	3.85E-02	-	-	-
12	55908	15362	6.61E-02	43876	16325	7.40E-02	39146	10925	5.72E-02	-	-	-
13	4088	18137	1.01E-02	23437	5894	3.25E-02	19132	6372	3.05E-02	-	-	-
14	21366	6732	3.31E-02	19910	6726	3.20E-02	15233	5033	2.42E-02	11741	4484	2.01E-02
15	21535	5868	3.10E-02	21988	7474	3.55E-02	17080	5416	2.66E-02	15401	4787	2.37E-02
16	30576	9404	4.68E-02	26531	7474	4.18E-02	24282	9405	4.18E-02	19935	5992	3.02E-02
17	45711	16932	4.67E-02	30587	8108	4.36E-02	27646	8640	4.27E-02	25926	8711	4.16E-02
18	36293	7929	4.60E-02	31766	10421	5.03E-02	30646	8888	4.56E-02	25320	7213	3.74E-02
19	45920	22638	8.89E-02	14932	5844	2.58E-02	12546	5616	2.32E-02	11386	4448	1.97E-02
20	67351	19398	9.97E-02	25475	6562	3.58E-02	21787	5570	3.05E-02	18149	4819	2.59E-02
21	93411	30403	1.47E-01	78091	2145	4.17E-02	35364	10432	5.31E-02	28236	8042	4.17E-02

(Continued)

Table 2 Count rate of heart from image scanning at the interval time

Patient	Time (minute)			Time (minute)			Time (minute)		
	0-10		Activity	30-40		Activity	60-70		Activity
	AP	PA	(mCi)	AP	PA	(mCi)	AP	PA	(mCi)
1	94605	49355	1.18E+00	22557	21128	3.77E-01	20390	971	7.68E-02
2	116344	58448	1.42E+00	22158	18281	3.47E-01	16459	11078	2.33E-01
3	54063	20805	5.79E-01	21780	19840	3.59E-01	14856	12901	2.39E-01
4	130822	57337	1.49E+00	38809	27224	5.61E-01	25399	16526	3.54E-01
5	45567	13848	4.34E-01	28875	17527	3.88E-01	17980	19113	3.20E-01
6	135971	56434	1.51E+00	18225	18528	3.17E-01	16196	15695	2.75E-01
7	103105	60039	1.36E+00	37105	22666	5.00E-01	46646	19776	5.24E-01
8	149386	61980	1.66E+00	42612	19560	4.98E-01	37085	10676	3.43E-01
9	88694	39510	1.02E+00	43175	16369	4.59E-01	33506	16835	4.10E-01
10	90323	53216	1.20E+00	28117	12780	3.27E-01	21325	9219	2.42E-01
11	143762	35707	1.24E+00	33837	18506	4.32E-01	27858	9531	2.81E-01
12	80881	65633	1.26E+00	23127	14071	3.11E-01	15846	10657	2.24E-01
13	103245	36944	1.07E+00	23196	10432	2.68E-01	20616	7466	2.14E-01
14	40493	36815	6.66E-01	15221	10840	2.22E-01	23427	11438	2.83E-01
15	74228	32026	8.41E-01	17063	10964	2.36E-01	19308	8619	2.23E-01
16	81812	44568	1.04E+00	-	-	-	12601	12098	2.13E-01
17	83383	33827	9.17E-01	35918	14545	3.94E-01	31100	12994	3.47E-01
18	63221	32115	7.78E-01	33318	9905	3.14E-01	23772	8169	2.40E-01
19	-	-	-	18522	13111	2.69E-01	15115	9094	2.02E-01
20	-	-	-	30695	12654	3.40E-01	26191	11380	2.98E-01
21	-	-	-	-	-	-	-	-	-

(Continued)

Table 3 Count rate of liver from image scanning at the interval time

Patient	Time (minute)			Time (minute)		
	0-10		Activity	30-40		Activity
	AP	PA	(mCi)	AP	PA	(mCi)
1	169036	130239	1.39E+00	77260	22027	3.86E-01
2	57685	51385	5.09E-01	-	-	-
3	66986	24041	3.75E-01	30480	24958	2.58E-01
4	87311	61301	6.84E-01	44647	31466	3.50E-01
5	18241	24619	1.98E-01	47644	34526	3.79E-01
6	112538	98641	9.85E-01	32644	26270	2.74E-01
7	84298	68246	7.09E-01	16963	37655	2.36E-01
8	173859	69373	1.03E+00	73647	22419	3.80E-01
9	78595	39339	5.20E-01	56438	33988	4.09E-01
10	109963	75741	8.53E-01	54527	33312	3.98E-01
11	76507	72021	6.94E-01	44843	32437	3.57E-01
12	80586	55232	6.24E-01	37124	27572	2.99E-01
13	81289	57433	6.39E-01	61863	26046	3.75E-01
14	53735	35931	4.11E-01	32005	15106	2.06E-01
15	59862	32327	4.11E-01	34194	21581	2.54E-01
16	74756	43156	5.31E-01	24932	16954	1.92E-01
17	98379	56561	6.97E-01	38784	30100	3.19E-01
18	84588	56987	6.49E-01	41707	23694	2.94E-01
19	-	-	-	24269	18511	1.98E-01
20	-	-	-	29369	20600	2.30E-01
21	-	-	-	-	-	-

(Continued)

Table 4 Count rate of kidney from image scanning at the interval time

Patient	Time (minute)			Time (minute)		
	0-10		Activity	30-40		Activity
	AP	PA	(mCi)	AP	PA	(mCi)
1	24927	39939	5.18E-01	13160	12445	2.10E-01
2	8647	25303	2.43E-01	7898	12444	1.63E-01
3	14894	16294	2.56E-01	4675	5325	8.19E-02
4	15021	26298	3.26E-01	10647	12411	1.89E-01
5	10755	16685	2.20E-01	18313	27307	3.67E-01
6	5820	23051	1.90E-01	7665	9615	1.41E-01
7	19769	34653	4.30E-01	13422	24078	2.95E-01
8	46621	38144	6.92E-01	14461	17734	2.63E-01
9	22092	18493	3.32E-01	16489	8745	1.97E-01
10	11814	16693	2.31E-01	9791	11575	1.75E-01
11	22682	18444	3.36E-01	5469	8833	1.14E-01
12	17536	17156	2.85E-01	14056	14601	2.35E-01
13	19992	14811	2.83E-01	7402	8741	1.32E-01
14	9320	12563	1.78E-01	3947	3548	6.14E-02
15	8558	15962	1.92E-01	10776	3862	1.06E-01
16	11799	11355	1.90E-01	7442	6760	1.16E-01
17	13643	17089	2.51E-01	9802	5830	1.24E-01
18	17953	16589	2.83E-01	15461	9630	2.00E-01
19	-	-	-	-	-	-
20	-	-	-	-	-	-
21	-	-	-	-	-	-

(Continued)

Table 5 Count rate of bladder from image scanning at the interval time

Patient	Time (minute)			Time (minute)			Time (minute)		
	0-10		Activity	30-40		Activity	60-70		Activity
	AP	PA	(mCi)	AP	PA	(mCi)	AP	PA	(mCi)
1	29387	18810	7.13E-02	76395	26059	1.35E-01	105621	39407	1.96E-01
2	7786	5953	2.07E-02	29047	24562	8.10E-02	28969	21831	7.63E-02
3	4601	1868	8.89E-03	37631	17316	7.74E-02	40666	23875	9.45E-02
4	10398	13179	3.55E-02	30153	16361	6.74E-02	60753	24240	1.16E-01
5	8749	5719	2.15E-02	41658	36638	1.19E-01	23886	19362	6.52E-02
6	6583	4206	1.60E-02	31549	17717	7.17E-02	64772	46926	1.67E-01
7	13258	5014	2.47E-02	75434	36062	1.58E-01	86402	37073	1.72E-01
8	27676	17315	6.64E-02	117181	28083	1.74E-01	23140	10344	4.69E-02
9	10005	3985	1.92E-02	113082	42499	2.10E-01	123998	45451	2.28E-01
10	8161	3629	1.65E-02	72112	25465	1.30E-01	112713	38885	2.01E-01
11	15937	9352	3.70E-02	106814	36204	1.89E-01	111208	37574	1.96E-01
12	9849	2412	1.48E-02	120324	23205	1.60E-01	146805	15501	1.45E-01
13	1943	852	3.90E-03	75866	22096	1.24E-01	101036	28684	1.63E-01
14	2641	3279	8.93E-03	62520	9218	7.28E-02	80283	32931	1.56E-01
15	13961	13567	4.17E-02	101531	36039	1.83E-01	-	-	-
16	9756	9118	2.86E-02	-	-	-	124395	23365	1.64E-01
17	16973	18282	5.34E-02	63777	23479	1.17E-01	94444	31384	1.65E-01
18	4078	2230	9.15E-03	46297	14308	7.81E-02	69854	20303	1.14E-01
19	-	-	-	22538	11904	4.97E-02	34186	13229	6.45E-02
20	-	-	-	117549	42001	2.13E-01	180133	57511	3.09E-01
21	-	-	-	-	-	-	13194	9041	3.31E-02

(Continued)

Table 6 Count rate of stomach from image scanning at the interval time

Patient	Time (minute)			Time (minute)			Time (minute)			Time (minute)		
	0-10		Activity	30-40		Activity	60-70		Activity	90-100		Activity
	AP	PA	(mCi)	AP	PA	(mCi)	AP	PA	(mCi)			(mCi)
1	85552	19542	1.16E-01	189322	102442	3.94E-01	200193	107450	4.15E-01	-	-	-
2	52080	21574	9.49E-02	58683	27823	1.14E-01	75035	26480	1.26E-01	-	-	-
3	44314	20634	8.56E-02	30345	20673	7.09E-02	40344	15105	6.99E-02	-	-	-
4	55352	34891	1.24E-01	52815	30917	1.14E-01	64437	36060	1.36E-01	-	-	-
5	35657	7616	4.66E-02	79341	23017	1.21E-01	70662	18684	1.03E-01	-	-	-
6	57459	29854	1.17E-01	48823	24612	9.81E-02	49451	22858	9.52E-02	-	-	-
7	33311	26712	8.44E-02	221137	88531	3.96E-01	248438	126736	5.02E-01	-	-	-
8	71139	22213	1.13E-01	171187	28083	1.96E-01	23140	10344	4.38E-02	-	-	-
9	67480	38284	1.44E-01	203965	96184	3.96E-01	239491	102369	4.43E-01	-	-	-
10	33279	16572	6.65E-02	153386	77878	3.09E-01	117813	59938	2.38E-01	-	-	-
11	-	-	-	234253	115618	4.66E-01	224727	97349	4.19E-01	-	-	-
12	-	-	-	124942	47774	2.19E-01	111739	91323	2.86E-01	-	-	-
13	-	-	-	95321	49311	1.94E-01	139004	61184	2.61E-01	-	-	-
14	-	-	-	134951	57599	2.50E-01	167706	67716	3.02E-01	146832	47349	2.36E-01
15	-	-	-	139014	62074	2.63E-01	157600	61923	2.80E-01	150200	56532	2.61E-01
16	-	-	-	-	-	-	56725	30723	1.18E-01	71757	45797	1.62E-01
17	-	-	-	183352	85966	3.55E-01	213263	91628	3.96E-01	221827	90591	4.01E-01
18	-	-	-	168692	88205	3.45E-01	190591	104265	3.99E-01	168750	108689	3.83E-01
19	-	-	-	120484	65591	2.52E-01	119753	55367	2.30E-01	118352	48496	2.14E-01
20	-	-	-	152259	71071	2.94E-01	147030	75226	2.98E-01	155121	59362	2.72E-01
21	-	-	-	-	-	-	-	-	-	-	-	-

(Continued)

Table 7 Count rate of parotic gland from image scanning at the interval time

Patient	Time (minute)			Time (minute)			Time (minute)		
	0-10		Activity	30-40		Activity	60-70		Activity
	AP	PA	(mCi)	AP	PA	(mCi)	AP	PA	(mCi)
1	24018	16275	5.34E-02	13325	12567	3.57E-02	25020	22445	6.54E-02
2	27225	20772	3.69E-02	18990	12870	4.31E-02	6006	6223	1.69E-02
3	11672	16649	3.40E-02	5901	7331	1.81E-02	6397	4524	1.48E-02
4	18284	10528	3.83E-02	13020	9487	3.07E-02	10960	7845	2.56E-02
5	12166	21557	3.11E-02	10309	9847	2.78E-02	15225	9984	3.40E-02
6	6294	11254	6.16E-02	14440	13012	3.78E-02	17698	10578	3.77E-02
7	28741	23586	5.82E-02	20124	17506	5.18E-02	15782	11292	3.68E-02
8	19189	21764	4.19E-02	14933	7029	2.83E-02	7972	6431	1.98E-02
9	32270	31522	6.79E-02	18413	15666	4.68E-02	14400	15867	4.17E-02
10	18224	33593	5.46E-02	14586	8879	3.14E-02	11393	9893	2.93E-02
11	14353	34753	3.83E-02	11665	14879	3.63E-02	10750	11845	3.11E-02
12	20963	24695	5.13E-02	17317	9090	3.46E-02	7702	1789	1.02E-02
13	20344	42411	3.45E-02	10349	6640	2.29E-02	5202	4415	1.32E-02
14	14317	8483	3.04E-02	8580	7932	2.28E-02	5739	5817	1.59E-02
15	12534	9426	3.00E-02	13868	7048	2.73E-02	7272	6096	1.84E-02
16	11255	10370	2.98E-02	-	-	-	7721	5958	1.87E-02
17	18422	17148	2.99E-02	9248	6678	2.17E-02	12756	6624	2.54E-02
18	26397	18387	5.98E-02	6813	6034	1.77E-02	6749	7384	1.95E-02
19	13814	10661	3.35E-02	8444	6034	1.97E-02	5386	5800	1.54E-02
20	35664	22381	7.79E-02	22099	19300	5.70E-02	15639	13205	3.96E-02
21	19500	28238	6.47E-02	-	-	-	9808	7876	2.42E-02

(Continued)

Table 8 Count rate of nasal from image scanning at the interval time

Patient	Time (minute)			Time (minute)			Time (minute)			Time (minute)		
	0-10		Activity	30-40		Activity	60-70		Activity	90-100		Activity
	AP	PA	(mCi)	AP	PA	(mCi)	AP	PA	(mCi)			(mCi)
1	7595	3144	0.013192	36764	7017	0.044303	65983	6564	0.057405	-	-	-
2	19494	1937	0.009547	20473	1326	0.014372	21746	2109	0.01868	-	-	-
3	-	-	-	-	-	-	-	-	-	-	-	-
4	8145	3237	0.014163	12236	2201	0.014315	17542	5787	0.027792	-	-	-
5	5927	3329	0.008539	24324	3166	0.024206	27759	5242	0.033273	-	-	-
6	1062	1244	0.008413	5141	2055	0.008966	9787	1199	0.009449	-	-	-
7	8006	2494	0.009988	32775	1772	0.021021	52299	4968	0.044461	-	-	-
8	5624	1575	0.006102	26143	1748	0.018646	16252	4224	0.022854	-	-	-
9	15390	10841	0.027506	22832	7077	0.035063	26539	5852	0.034375	-	-	-
10	14810	10960	0.02811	15411	5415	0.025198	30570	5360	0.035308	-	-	-
11	7401	2550	0.007446	29111	5516	0.034953	38666	6631	0.044167	-	-	-
12	18717	3971	0.019456	32323	4262	0.032375	31885	4276	0.032208	-	-	-
13	15599	3494	0.008667	20922	2924	0.021574	31040	2424	0.023926	-	-	-
14	12090	1119	0.010146	19098	2658	0.019653	21789	4225	0.026465	26294	7420	0.038528
15	5980	548	0.004993	14582	1859	0.014361	14316	2363	0.016043	19350	2504	0.0192
16	14070	810	0.009312	-	-	-	23944	2987	0.023327	28571	3602	0.027982
17	39550	7387	0.028722	24694	4367	0.028644	30326	3031	0.026445	33188	4599	0.034078
18	22659	957	0.012634	10871	1781	0.012137	10189	1177	0.009552	15108	1046	0.010965
19	11693	3456	0.017535	13325	1099	0.010556	14164	1572	0.013016	16698	1521	0.013901
20	8217	3079	0.013874	14804	1789	0.014195	16069	1808	0.014868	16298	2017	0.015815
21	11737	5327	0.021811	-	-	-	11917	1084	0.009914	15029	1989	0.015081

(Continued)

Table 9 Thyroid Activity Percentage

Patient	% Activity in interval time			
	0-10 (min)	30-40 (min)	60-70 (min)	90-100 (min)
1	1.18	4.41	1.74	-
2	0.37	0.33	0.14	-
3	21.62	31.30	24.21	-
4	2.32	2.16	1.97	-
5	0.71	0.53	0.58	-
6	40.09	45.37	32.42	-
7	0.12	0.12	0.09	-
8	1.00	1.17	1.08	-
9	2.81	2.66	2.34	-
10	3.67	2.70	2.15	-
11	1.42	1.38	1.05	-
12	1.65	1.85	1.43	-
13	0.40	1.30	1.22	-
14	1.11	1.08	0.81	0.68
15	1.06	1.21	0.91	0.81
16	1.57	1.47	1.40	1.01
17	1.73	1.61	1.58	1.54
18	1.62	1.77	1.60	1.31
19	5.36	1.56	1.40	1.19
20	3.72	1.34	1.14	0.97
21	5.68	-	2.05	1.61

Table 10 Heart Activity Percentage

Patient	% Activity in interval time			
	0-10 (min)	30-40 (min)	60-70 (min)	90-100 (min)
1	35.76	11.42	2.33	-
2	48.74	11.90	7.98	-
3	23.59	14.62	9.74	-
4	48.62	18.25	11.50	-
5	9.68	8.67	7.14	-
6	30.24	6.34	5.50	-
7	33.35	12.29	12.88	-
8	40.08	12.03	8.29	-
9	26.02	11.69	10.44	-
10	48.64	13.30	9.84	-
11	33.73	11.78	7.67	-
12	31.44	7.79	5.61	-
13	42.57	10.72	8.55	-
14	22.41	7.46	9.50	-
15	28.79	8.08	7.62	-
16	34.93	0.00	7.14	-
17	33.95	14.61	12.85	-
18	27.32	11.02	8.45	-
19	-	16.20	12.19	-
20	-	12.70	11.13	-
21	-	-	-	-

(Continued)

Table 11 Liver Activity Percentage

Patient	% Activity in interval time			
	0-10 (min)	30-40 (min)	60-70 (min)	90-100 (min)
1	42.06	11.70	-	-
2	17.43	0.00	-	-
3	15.29	10.51	-	-
4	22.25	11.40	-	-
5	4.42	8.47	-	-
6	19.70	5.48	-	-
7	17.42	5.80	-	-
8	24.78	9.17	-	-
9	13.24	10.43	-	-
10	34.69	16.20	-	-
11	18.93	9.73	-	-
12	15.60	7.48	-	-
13	25.51	14.99	-	-
14	13.82	6.91	-	-
15	14.07	8.69	-	-
16	17.80	6.44	-	-
17	25.83	11.83	-	-
18	22.81	10.33	-	-
19	-	11.94	-	-
20	-	8.59	-	-
21	-	-	-	-

Table 12 Kidney Activity Percentage

Patient	% Activity in interval time			
	0-10 (min)	30-40 (min)	60-70 (min)	90-100 (min)
1	15.71	6.37	-	-
2	8.32	5.57	-	-
3	10.42	3.34	-	-
4	10.62	6.14	-	-
5	4.91	8.20	-	-
6	3.80	2.82	-	-
7	10.56	7.25	-	-
8	16.71	6.35	-	-
9	8.45	5.02	-	-
10	9.37	7.11	-	-
11	9.16	3.11	-	-
12	7.12	5.88	-	-
13	11.28	5.27	-	-
14	5.98	2.07	-	-
15	6.57	3.62	-	-
16	6.37	3.90	-	-
17	9.29	4.60	-	-
18	9.96	7.04	-	-
19	-	-	-	-
20	-	-	-	-
21	-	-	-	-

(Continued)

Table 13 Bladder Activity Percentage

Patient	% Activity in interval time			
	0-10 (min)	30-40 (min)	60-70 (min)	90-100 (min)
1	2.16	1.70	1.82	-
2	0.71	2.07	0.05	-
3	0.30	2.35	0.46	-
4	1.22	0.82	1.61	-
5	0.73	3.31	1.82	-
6	0.55	1.91	3.24	-
7	0.85	4.56	0.35	-
8	2.27	3.23	4.24	-
9	0.66	6.55	0.59	-
10	0.57	3.88	2.42	-
11	1.27	5.13	0.25	-
12	0.51	4.98	-	-
13	0.13	4.12	1.34	-
14	0.31	1.96	2.13	0.66
15	1.43	4.61	6.28	-
16	0.98	0.98	5.60	0.56
17	1.83	1.62	1.62	0.28
18	0.31	2.35	1.23	1.41
19	-	1.70	0.41	1.61
20	-	7.30	3.24	0.49
21	-	-	4.28	2.13

Highlight shows the patient who urinate while examination

Table 14 Stomach Activity Percentage

Patient	% Activity in interval time			
	0-10 (min)	30-40 (min)	60-70 (min)	90-100 (min)
1	3.51	11.95	12.59	-
2	3.25	3.92	4.32	-
3	3.49	2.89	2.85	-
4	4.05	3.72	4.44	-
5	1.04	2.70	2.30	-
6	2.34	1.96	1.90	-
7	2.07	9.73	12.34	-
8	2.72	4.74	1.06	-
9	3.66	10.10	11.29	-
10	2.70	12.58	9.67	-
11	-	12.71	11.42	-
12	-	5.47	7.15	-
13	-	7.75	10.42	-
14	-	8.39	10.15	7.94
15	-	9.00	9.57	8.92
16	-	-	3.96	5.44
17	-	13.16	14.65	14.86
18	-	12.13	14.02	13.47
19	-	15.16	13.88	12.92
20	-	10.99	11.12	10.14
21	-	-	4.28	2.13

(Continued)

Table 15 Parotic gland Activity Percentage

Patient	% Activity in interval time			
	0-10 (min)	30-40 (min)	60-70 (min)	90-100 (min)
1	1.62	1.08	1.98	-
2	1.27	1.48	0.58	-
3	1.39	0.74	0.60	-
4	1.24	1.00	0.83	-
5	0.70	0.62	0.76	-
6	1.23	0.76	0.75	-
7	1.43	1.27	0.90	-
8	1.01	0.68	0.48	-
9	1.73	1.19	1.06	-
10	2.22	1.28	1.19	-
11	1.04	0.99	0.85	-
12	1.28	0.87	0.26	-
13	1.38	0.91	0.53	-
14	1.02	0.77	0.54	0.47
15	1.03	0.93	0.63	0.68
16	1.00	-	0.63	0.70
17	1.11	0.80	0.94	0.77
18	2.10	0.62	0.68	0.66
19	2.02	1.19	0.93	0.60
20	2.91	2.13	1.48	1.12
21	2.50	-	0.94	0.53

Table 16 Nasal Activity Percentage

Patient	% Activity in interval time			
	0-10 (min)	30-40 (min)	60-70 (min)	90-100 (min)
1	0.40	1.34	1.74	-
2	0.33	0.49	0.64	-
3	-	-	-	-
4	0.46	0.47	0.90	-
5	0.19	0.54	0.74	-
6	0.17	0.18	0.19	-
7	0.25	0.52	1.09	-
8	0.15	0.45	0.55	-
9	0.70	0.89	0.88	-
10	1.14	1.02	1.44	-
11	0.20	0.95	1.20	-
12	0.49	0.81	0.81	-
13	0.35	0.86	0.96	-
14	0.34	0.66	0.89	1.30
15	0.17	0.49	0.55	0.66
16	0.31	-	0.78	0.94
17	1.06	1.06	0.98	1.26
18	0.44	0.43	0.34	0.39
19	1.06	0.64	0.78	0.84
20	0.52	0.53	0.56	0.59
21	0.84	-	0.38	0.58

(Continued)

Table 17 Activity percentage resume for all organs

Organ	Activity percentage in interval time			
	0-10 min	30-40 min	60-70 min	90 -100 min
Thyroid	1.15 ± 0.47	1.30 ± 0.25	1.24 ± 0.26	1.14 ± 0.33
Parotic	1.49 ± 0.57	0.97 ± 0.42	0.84 ± 0.38	0.69 ± 0.20
Nasal	0.32 ± 0.13	0.58 ± 0.32	0.80 ± 0.38	0.88 ± 0.30
Heart	33.33 ± 10.12	11.62 ± 3.07	8.82 ± 2.66	-
Liver	17.85 ± 3.78	8.37 ± 2.12	-	-
Stomach	2.88 ± 0.90	11.47 ± 2.21	12.07 ± 2.21	11.38 ± 2.77
Kidney	7.74 ± 2.27	0.90 ± 0.28	-	-
Bladder	0.36 ± 0.17	2.76 ± 0.98	1.80 ± 0.99	0.68 ± 0.54

Appendix E: Pharmacokinetics Data

Table 1 Thyroid activity percentage of 3 normal patients

Time (s)	% Activity of patient				
	1	2	3	Mean	SD
2	1.14	1.13	1.48	1.14	0.01
4	2.41	2.49	3.59	2.45	0.06
6	3.85	4.00	5.95	3.93	0.10
8	8.04	5.58	8.52	6.81	1.73
10	10.44	7.25	11.18	8.84	2.26
12	8.57	8.92	13.91	8.74	0.25
14	10.21	10.62	16.69	10.41	0.28
16	11.88	12.34	19.50	12.11	0.32
18	13.54	14.04	22.27	13.79	0.35
20	15.21	10.41	25.07	12.81	3.40
30	1.55	1.33	0.00	1.44	0.16
60	1.39	1.13	2.05	1.26	0.18
90	1.18	0.96	0.00	1.07	0.16
120	1.03	0.86	1.61	0.94	0.12

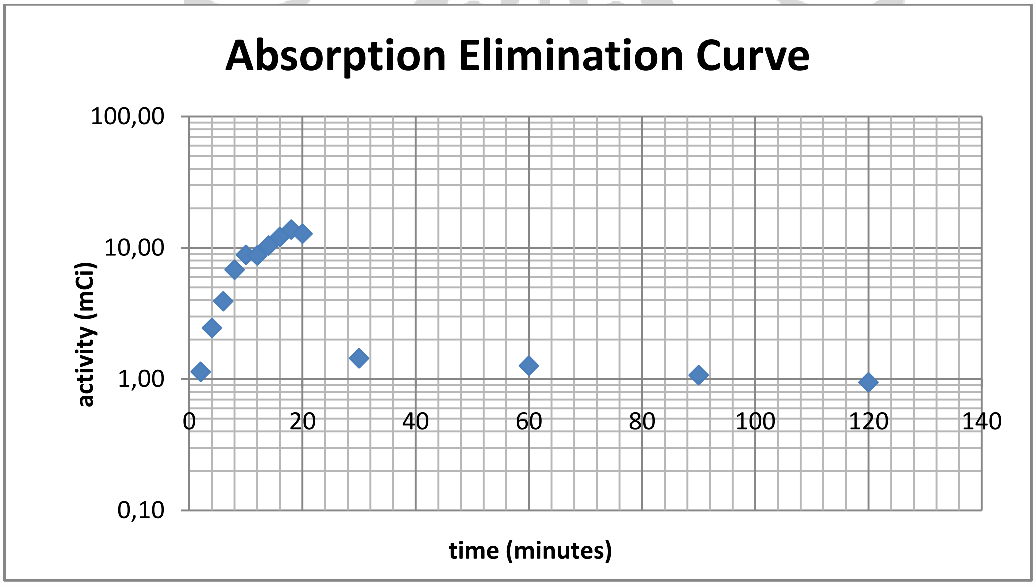

Figure 1 One compartment model of pharmacokinetics curve

(Continued)

<u>Information</u>

Elimination rate in human body:

$$k = \frac{\ln(A_{t,1}) - \ln(A_{t,2})}{t_2 - t_1} = \frac{\ln(\%A_{t,1}) - \ln(\%A_{t,2})}{t_2 - t_1}$$

Effective half life:

$$T_{1/2} = \frac{\ln 2}{k}$$

Table 2 Normal patient pharmacokinetics data for obtaining effective half life of thyroid

Patient	% Activity in time (minute)			k	$T_{1/2}$
	6	30	60	(/minute)	(minute)
1	3.67E+00	2.70E+00	2.15E+00	2.10E-06	9.19E+01
2	1.65E+00	1.85E+00	1.43E+00	2.39E-06	8.06E+01
3	1.11E+00	1.08E+00	8.15E-01	2.16E-06	8.91E+01
4	1.06E+00	1.21E+00	9.10E-01	1.86E-06	1.04E+02
5	1.57E+00	1.47E+00	1.40E+00	1.73E-06	1.11E+02
6	1.62E+00	1.77E+00	1.60E+00	1.38E-06	1.40E+02
7	5.36E+00	1.56E+00	1.40E+00	1.26E-06	1.53E+02
8	3.72E+00	1.34E+00	1.14E+00	1.50E-06	1.28E+02
			Mean	1.80E-06	1.12E+02
			SD	4.02E-07	2.59E+01

(Continued)

Table 3 Several organs elimination rate of each patient

Patient	*k* (/minute)					
	Thyroid	Heart	Liver	Kidney	Bladder	Stomach
1	3.10E-02	4.55E-02	4.27E-02	3.01E-02	-2.27E-03	-
2	2.86E-02	3.02E-02	-	1.34E-02	1.24E-01	-
3	8.56E-03	1.47E-02	1.25E-02	3.79E-02	5.44E-02	-
4	3.07E-03	2.40E-02	2.23E-02	1.83E-02	-2.25E-02	-
5	-3.01E-03	5.07E-03	-2.17E-02	-1.71E-02	1.99E-02	-
6	1.12E-02	2.84E-02	4.27E-02	9.94E-03	-1.76E-02	-
7	9.59E-03	1.59E-02	3.67E-02	1.25E-02	8.56E-02	-
8	2.67E-03	2.63E-02	3.31E-02	3.23E-02	-9.07E-03	-
9	4.27E-03	1.52E-02	7.95E-03	1.74E-02	8.02E-02	-
10	7.59E-03	2.66E-02	2.54E-02	9.20E-03	1.57E-02	-
11	9.11E-03	2.47E-02	2.22E-02	3.60E-02	1.01E-01	-
12	8.58E-03	2.87E-02	2.45E-02	6.38E-03	-	-
13	2.12E-03	2.68E-02	1.77E-02	2.54E-02	3.74E-02	-
14	9.59E-03	1.43E-02	2.31E-02	3.54E-02	-2.77E-03	8.19E-03
15	9.50E-03	2.22E-02	1.61E-02	1.99E-02	-1.03E-02	2.34E-03
16	1.63E-03	2.65E-02	3.39E-02	1.64E-02	-5.81E-02	-1.06E-02
17	6.27E-04	1.62E-02	2.60E-02	2.34E-02	-	-4.74E-04
18	3.37E-03	1.96E-02	2.64E-02	1.16E-02	2.16E-02	1.33E-03
19	3.61E-03	-	-	-	4.74E-02	2.39E-03
20	5.39E-03	-	-	-	2.71E-02	3.08E-03
21	8.05E-03	-	-	-	2.33E-02	2.33E-02

Highlight shows the patient who urinate while examination

Appendix F: Internal Dose of Organs

Information

Cumulative activity was calculated by using Trapezoidal Rule for numerical integration

$$\tilde{A}_h = \frac{1}{2}[A_j + (A_j + 1)][(t_j + 1) - t_j] + 1.443 A_n T_p$$

A_j= activity (µCi) measured at $t = t_j$
A_n = activity (µCi) at time of last measurement (t_n)
T_p = physical half life (hour)

Table 1 Cumulative activity of source organ

Patient	Cumulative Activity in Organs (µCi hr)					
	Stomach	Heart	Liver	Kidney	Bladder	Thyroid
1	60.79	22.43	54.70	49.07	52.92	37.42
2	48.90	32.61	-	46.62	43.63	15.19
3	43.10	32.66	50.82	40.51	45.38	58.74
4	49.68	36.80	53.69	48.00	47.49	41.43
5	46.91	35.34	54.11	53.85	42.47	32.85
6	46.25	34.09	51.57	45.28	50.69	67.98
7	62.47	40.31	50.18	52.05	51.60	13.46
8	39.61	36.47	54.50	51.13	39.96	34.94
9	61.44	37.93	55.01	48.40	54.34	45.64
10	55.37	32.88	54.88	47.24	52.81	40.23
11	55.49	34.47	53.84	43.53	53.03	37.01
12	51.89	32.15	52.25	49.94	49.92	37.24
13	51.05	31.58	54.28	44.79	50.56	31.43
14	55.86	33.89	48.82	37.87	49.94	32.35
15	56.73	31.80	50.70	42.74	-	30.21
16	46.67	30.23	48.28	43.58	48.22	35.77
17	61.02	36.26	52.86	44.21	51.19	37.85
18	60.60	32.69	52.11	48.50	47.13	35.13
19	54.78	2053.81	-	0.00	38.21	32.00
20	57.18	2983.78	-	0.00	52.57	34.74
21	-	-	-	0.00	38.47	38.47

(Continued)

Information

Internal dose of target organ (mGy) was calculated by using MIRD method with absorbed dose per cumulated activity, *S* value from AAPM Task Group No.5 (AAPM, 1992).

$$\overline{D}(r_k \leftarrow r_h) = \widetilde{A}_h \sum S(r_k \leftarrow r_h)$$

Table 2 Internal dose of target organs

Patient	Target Organ Dose (rad)					
	Stomach	Heart	Liver	Kidney	Bladder	Thyroid
1	9.94E-03	2.82E-03	4.23E-03	1.16E-02	2.91E-02	1.28E-01
2	7.95E-03	3.49E-03	1.06E-03	1.08E-02	2.35E-02	5.20E-02
3	5.70E-03	2.79E-03	3.09E-03	7.91E-03	2.10E-02	1.27E-01
4	8.26E-03	4.14E-03	4.12E-03	1.13E-02	2.62E-02	1.42E-01
5	7.83E-03	3.98E-03	4.09E-03	1.26E-02	2.36E-02	1.12E-01
6	6.13E-03	2.92E-03	3.21E-03	8.81E-03	2.34E-02	1.48E-01
7	1.02E-02	4.51E-03	4.05E-03	1.23E-02	2.84E-02	4.61E-02
8	6.70E-03	4.05E-03	4.05E-03	1.19E-02	2.23E-02	1.20E-01
9	1.01E-02	4.32E-03	4.33E-03	1.15E-02	2.99E-02	1.56E-01
10	7.25E-03	2.86E-03	3.40E-03	9.22E-03	2.44E-02	8.73E-02
11	7.25E-03	2.97E-03	3.35E-03	8.55E-03	2.45E-02	8.03E-02
12	8.60E-03	3.70E-03	4.07E-03	1.18E-02	2.75E-02	1.27E-01
13	6.70E-03	2.74E-03	3.33E-03	8.75E-03	2.34E-02	6.82E-02
14	9.15E-03	3.85E-03	3.84E-03	9.13E-03	2.74E-02	1.11E-01
15	9.03E-03	3.57E-03	3.30E-03	9.90E-03	1.35E-03	1.03E-01
16	7.75E-03	3.47E-03	3.78E-03	1.03E-02	2.65E-02	1.22E-01
17	9.99E-03	4.13E-03	4.14E-03	1.06E-02	2.82E-02	1.29E-01
18	7.86E-03	2.85E-03	3.23E-03	9.43E-03	2.19E-02	7.63E-02
19	8.54E-03	3.28E-04	6.68E-04	4.48E-04	2.03E-02	1.09E-01
20	8.98E-03	3.68E-04	8.66E-04	5.45E-04	2.79E-02	1.19E-01
21	1.52E-04	7.57E-05	4.24E-04	2.01E-04	1.69E-02	8.35E-02

(Continued)

Information

Target organ dose per administered activity (mGy/mCi) was obtained by divided internal organ dose by administered activity.

$$\overline{D}/A_0 = \frac{\overline{D}(r_k \leftarrow r_h)}{A_0}$$

A_0 = administered activity (mCi)

Table 3 Target organ dose per administered activity

Patient	$(D_{rk} \leftarrow_{rh})/A_0$					
	Stomach	Heart	Liver	Kidney	Bladder	Thyroid
1	1.02E-01	2.22E-02	1.66E-02	3.68E-02	7.20E-01	3.88E-01
2	9.25E-02	3.65E-02	-	3.95E-02	8.23E-02	1.78E-01
3	7.80E-02	3.30E-02	1.67E-02	3.36E-02	7.75E-01	5.20E-01
4	8.92E-02	3.92E-02	1.75E-02	3.86E-02	6.94E-01	4.61E-01
5	5.78E-02	2.58E-02	1.21E-02	2.97E-02	5.22E-02	2.51E-01
6	4.11E-02	1.69E-02	8.33E-03	1.84E-02	4.25E-01	2.95E-01
7	8.47E-02	3.24E-02	1.24E-02	3.16E-02	5.69E-01	1.13E-01
8	5.26E-02	2.87E-02	1.31E-02	3.04E-02	5.29E-02	2.87E-01
9	8.64E-02	3.16E-02	1.41E-02	3.05E-02	6.21E-01	3.98E-01
10	1.00E-01	3.31E-02	1.80E-02	3.91E-02	8.99E-01	3.55E-01
11	6.72E-02	2.33E-02	1.19E-02	2.42E-02	6.06E-01	2.19E-01
12	7.17E-02	2.63E-02	1.31E-02	3.09E-02	6.87E-02	3.19E-01
13	9.06E-02	3.12E-02	1.75E-02	3.64E-02	8.46E-01	2.73E-01
14	1.04E-01	3.73E-02	1.65E-02	3.15E-02	7.54E-01	3.72E-01
15	1.07E-01	3.56E-02	1.74E-02	3.62E-02	-	3.54E-01
16	8.64E-02	3.31E-02	1.62E-02	3.61E-02	7.26E-01	4.10E-01
17	1.25E-01	4.39E-02	1.96E-02	4.05E-02	8.51E-01	4.80E-01
18	9.46E-02	2.84E-02	1.48E-02	3.47E-02	6.94E-01	2.68E-01
19	1.82E-01	-	-	-	1.03E+00	6.60E-01
20	1.18E-01	-	-	-	8.81E-01	4.44E-01
21	8.64E-02	-	-	-	-	3.23E-01
Mean	9.15E-02	3.10E-02	1.51E-02	3.33E-02	7.40E-01	3.38E-01
SD	3.00E-02	6.58E-03	2.91E-03	5.62E-03	1.52E-01	8.44E-02

Appendix G: Effective Dose Equivalent

<u>Information</u>

Effective dose equivalent (mSv) was calculated by using tissue weighting factor from ICRP (ICRP, 1987).

$$H_E = w_T H_T$$

w_T = the weighting factor for organ or tissue T
H_T = the mean dose equivalent in T (mGy)

Table 1 Weighting factors for calculation of effective dose equivalent (H_E)

Tissue	w_T
Gonads	0.25
Breast	0.15
Red bone marrow	0.12
Lungs	0.12
Thyroid	0.03
Bone surface	0.03
Remainder	0.30

Table 2 Effective dose equivalent per administered activity of this study

Organ	Dose per unit activity (mGy/mCi)	EDE (H_E) (mSv/mCi)
Stomach	9.15E-02	5.49E-03
Heart	3.10E-02	1.86E-03
Liver	1.50E-02	9.00E-04
Kidney	3.33E-02	2.00E-03
Bladder	7.40E-01	4.44E-02
Thyroid	3.38E-01	1.01E-02
Total Body	1.25E+00	6.48E-02

Appendix H: TLD measurement

Table 1 TLD conversion factor

Energy	140 keV
HVL	10.2 mmCu
mAs	0.5 mA; 74 seconds
Dose	2.2 mGy (3measurements)
Group	TLD CF (mGy/mCi)
1	5.60E-02
2	5.80E-02
3	6.60E-02

Table 2 Patient Measurements with TLD

Patient	Dose rate (mGy/min)			Dose rate/A0 (mGy/mCi min)		
	Thyroid	Stomach	Bladder	Thyroid	Stomach	Bladder
1	7.72E-03	7.13E-03	7.46E-03	1.72E-03	1.59E-03	1.67E-03
2	1.06E-02	1.11E-02	1.06E-02	2.90E-03	3.03E-03	2.90E-03
3	5.45E-03	6.06E-03	5.72E-03	1.36E-03	1.52E-03	1.43E-03
4	6.53E-03	6.87E-03	6.81E-03	3.93E-03	4.14E-03	4.10E-03
5	1.00E-02	7.13E-03	7.81E-03	3.74E-03	2.66E-03	2.92E-03
6	8.36E-03	9.09E-03	7.96E-03	3.23E-03	3.51E-03	3.08E-03
7	1.39E-02	2.20E-02	1.92E-02	5.54E-03	8.80E-03	7.66E-03
8	1.28E-02	1.30E-02	1.31E-02	4.29E-03	4.37E-03	4.41E-03
9	3.17E-02	3.47E-02	3.41E-02	1.09E-02	1.19E-02	1.17E-02
10	1.13E-02	1.39E-02	1.24E-02	4.17E-03	5.13E-03	4.61E-03
11	1.15E-02	1.27E-02	1.32E-02	3.86E-03	4.27E-03	4.43E-03
12	1.16E-02	1.47E-02	1.03E-02	4.06E-03	5.16E-03	3.63E-03
Mean	1.18E-02	1.32E-02	1.24E-02	4.14E-03	4.67E-03	4.37E-03
SD	6.77E-03	8.14E-03	7.78E-03	2.40E-03	2.98E-03	2.81E-03

Appendix I: Phantom Study

<u>Phantom design</u>

Dimension: 10 cm x 15 cm x 12 cm.

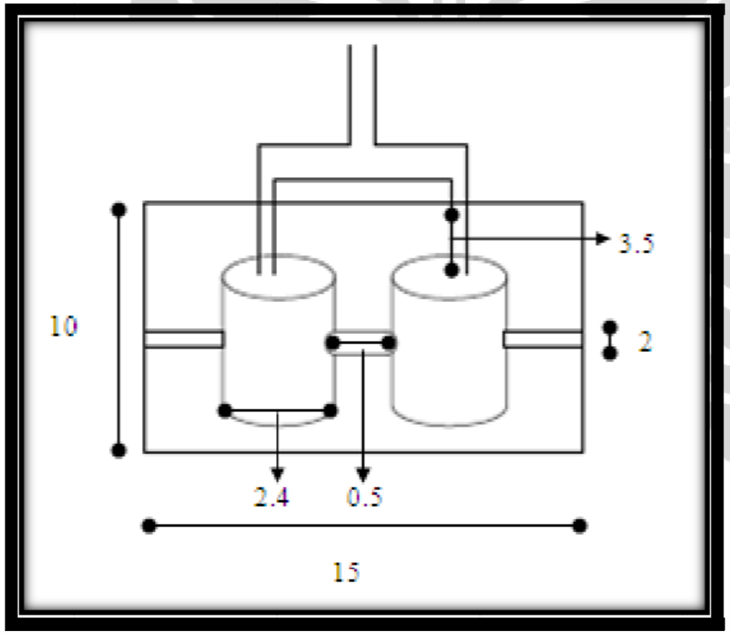

Figure 2. Dynamic Thyroid Phantom design
(with dimensions)

All dimensions in Figure 2 are in centi meter

(Continued)

Table 1 Elimination rate testing of phantom

Meas.	Time 6 minutes		Activity (mCi)	Time 30 minutes		Activity (mCi)	Time 60 minutes		Activity (mCi)	Time 90 minutes		Activity (mCi)	k (/minute)	$T_{1/2}$ (minute)
	AP	PA		AP	PA		AP	PA		AP	PA			
1	13736	3058	1.79E-02	41740	7836	5.00E-02	36314	6816	4.35E-02	29421	5299	3.45E-02	6.17E-03	112.26
2	13964	3176	1.84E-02	41098	7769	4.94E-02	33920	7552	4.43E-02	29009	5263	3.42E-02	6.15E-03	112.74
3	14015	3241	1.86E-02	43179	7865	5.10E-02	34149	7571	4.45E-02	30121	5402	3.53E-02	6.13E-03	113.05
4	13643	3097	1.80E-02	40969	7687	4.91E-02	33735	7511	4.40E-02	26734	5613	3.39E-02	6.18E-03	112.20
5	14091	3100	1.83E-02	40784	7665	4.89E-02	34500	7530	4.46E-02	26312	5662	3.38E-02	6.18E-03	112.23
												Mean	6.16E-03	112.49
												SD	1.95E-05	3.80E-01

Table 2 Internal dose of thyroid phantom

Meas.	$(\tilde{A}_h)$ (µCi hr)	$D(r_k \leftarrow r_h)$ (mGy)	Ao (mCi)	$D(r_k \leftarrow r_h)/Ao$ (mGy/mCi)
1	3.64E+01	7.89E-01	2.43	3.25E-01
2	3.63E+01	7.87E-01	2.47	3.19E-01
3	3.66E+01	7.93E-01	2.61	3.04E-01
4	3.62E+01	7.85E-01	2.27	3.46E-01
5	3.62E+01	7.84E-01	1.96	4.00E-01
			Mean	3.39E-01
			SD	3.76E-02

Appendix J: Informed Consent for Patient Agreement

INFORMED CONSENT

Tanggal : … / … /…

Yang bertanda tangan di bawah ini:

Nama :

TTL :

Alamat :

Bersama ini menyatakan telah memahami dan bersedia menjalani pemeriksaan **skintigrafi kelenjar tiroid dengan modalitas kedokteran nuklir** untuk keperluan penelitian Program Magister Fisika Pascasarjana FMIPA Universitas Indonesia, kekhususan Fisika Medis.

Pasien	Peneliti
( )	( )

GLOSSARY

AP (anterior - posterior)

CCF (count rate conversion factor)

CT (computerized tomography)

EDE (effective dose equivalent)

SD (surface dose)

LLI (lower large instentine)

MG (mean geometric)

PA (posterior – anterior)

ROI (region of interest)

SI (small instentine)

SPECT (single photon emission computerized tomography)

TLD (thermoluminisence dosimeter)

TLD(CF) (thermoluminisence dosimeter conversion factor)

TPS (treatment planning system)

ULI (upper large instentine)